

Structure Formation and Cosmology with high-z Clusters

Outline

Piero Rosati (ESO)

L1 : Introduction, observational techniques

- Observational definition, observable physical properties
- Methods for cluster searches - Cluster surveys
- Multi-wavelength observations of distant clusters

L2: Clusters as Cosmological Tools

- Constraining cosmological parameters with clusters
- The new population of high-z clusters

L3: Probing Dark Matter in Clusters

- Basics of gravitational lensing (strong and weak)
- Constraining DM density profiles in cores - Λ CDM predictions
- Clusters as gravitational telescopes

Gravitational Lensing as a powerful Cosmological diagnostic Tool

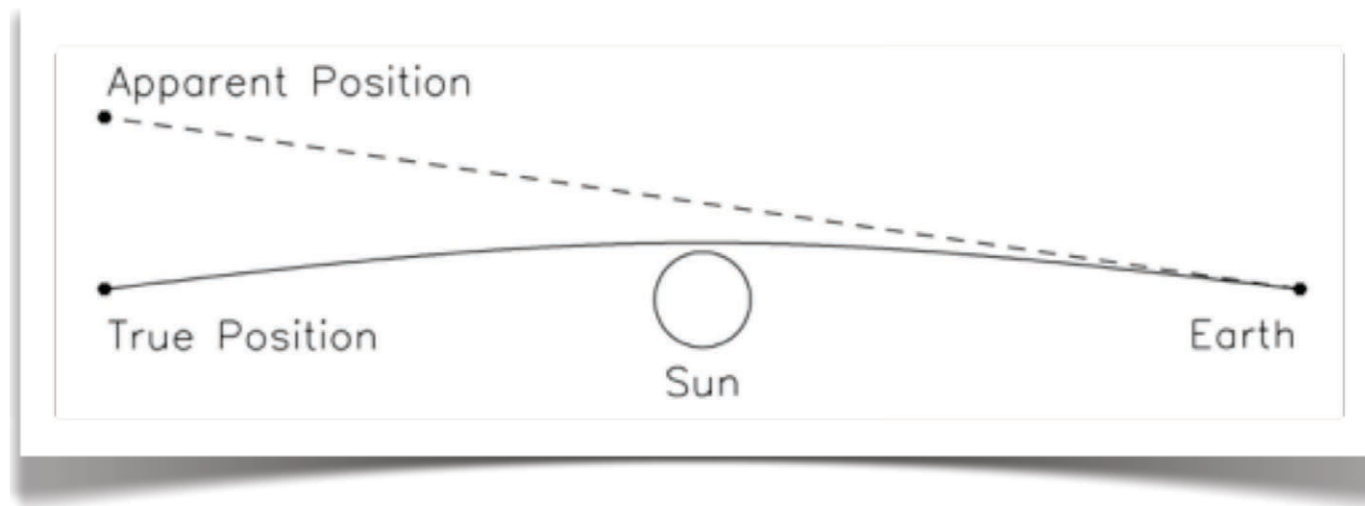
- 1) GL provides a direct probe of the (dark) matter distribution in the Universe (regardless of its composition and physical state):
 - Mass distribution in deep potential wells (inner mass profiles of massive galaxies and clusters) → stringent test of CDM scenario
 - Can give some (indirect) clues on the nature of DM (e.g. collisionless?)
 - Power spectrum, $P(k)$ on a wide range of scales (avoids dealing with ‘biasing’ when light is used as a tracer)

- 2) GL provides natural “gravitational telescopes”:
 - The magnification provided by massive systems in special serendipitous geometrical conditions allows the detection of faint distant sources whose identification would require the next generation of giant telescopes.
 - It allows spectroscopic studies well beyond the spec limit → redshift, properties such as SF rate and chemical composition of primordial galaxies, identification of the first stars

Brief historical perspective

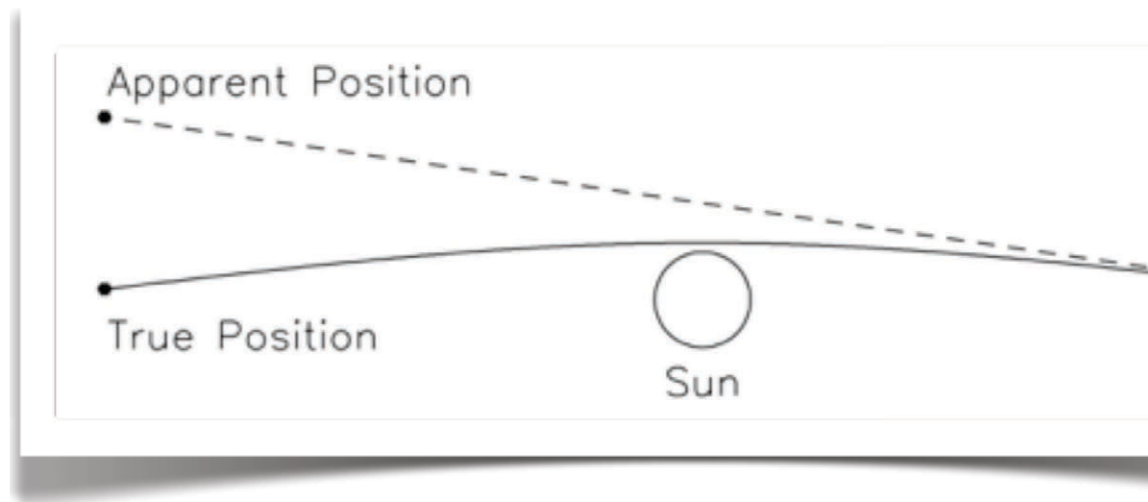
- Hypothesis of light deflection by Newtonian gravity goes back to Newton and Laplace, Soldner (1804) derives the classical deflection formula
- Einstein (1915) using GR equations finds a deflection angle with a factor of 2 higher than the classical formula (1.74" for the Sun)

$$\alpha = \frac{2GM}{c^2} \frac{1}{r}$$



Brief historical perspective

- Hypothesis of light deflection by Newtonian gravity goes back to Newton and Laplace, Soldner (1804) derives the classical deflection formula
$$\alpha = \frac{2GM}{c^2} \frac{1}{r}$$
- Einstein (1915) using GR equations finds a deflection angle with a factor of 2 higher than the classical formula (1.74" for the Sun)
- Eddington (1919) confirms the deflection prediction of stars near the solar limb



**LIGHTS ALL ASKEW
IN THE HEAVENS**

Men of Science More or Less
Agog Over Results of Eclipse
Observations.

EINSTEIN THEORY TRIUMPHS

Stars Not Where They Seemed
or Were Calculated to be,
but Nobody Need Worry.

A BO **NYT 1919** MEN

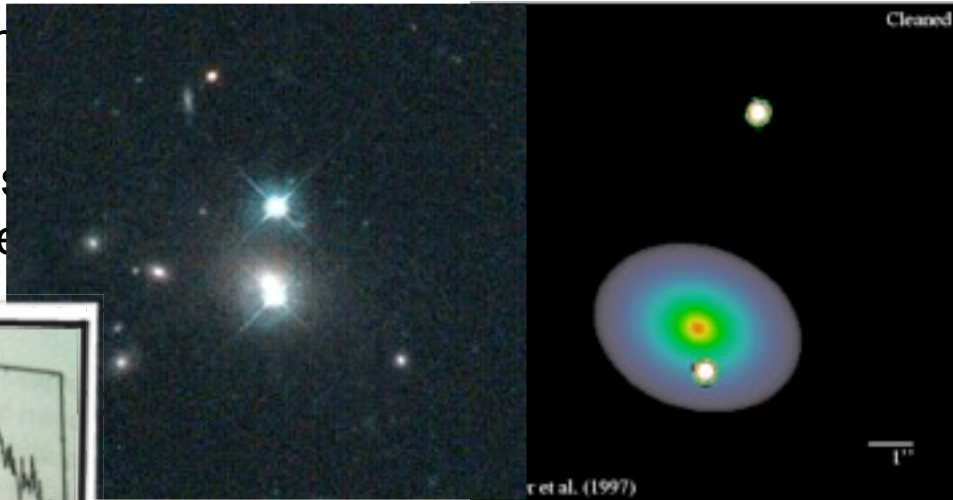
No More in All the World Could
Comprehend It, Said Einstein When
His Daring Publishers Accepted It.

Brief historical perspective

- Hypothesis of light deflection by Newtonian gravity goes back to Newton and Laplace, Soldner (1804) derives the classical deflection formula
$$\alpha = \frac{2GM}{c^2} \frac{1}{r}$$
- Einstein (1915) using GR equations finds a deflection angle with a factor of 2 higher than the classical formula (1.74" for the Sun)
- Eddington (1919) confirms the deflection prediction of stars near the solar limb
- Chwolson (1926) conceives the possibility of multiple images ("fictitious stars") of stars by a lensing stars, and even rings in symmetric geometry
- Einstein (1936) considers the same possibility (also rings) and concludes there is little chance to observe the effect for stellar-mass lenses..
- Zwicky (1937) using his new galaxy mass estimates ($\sim 4 \times 10^{11} M_{\odot}$) concluded:
 - lensing by galaxies can split images to large observable angles
 - this could be used to estimate galaxy masses
 - magnification can lead to access distant faint galaxies!
- Refsdal (1964): time delay from variability of multiple sources can be used to measure H_0 (if an accurate mass model is available..)

Brief historical perspective

- Hypothesis of light deflection by Newton and Laplace, Soldner
- Einstein (1915) used GR to predict deflection a factor of 2 higher



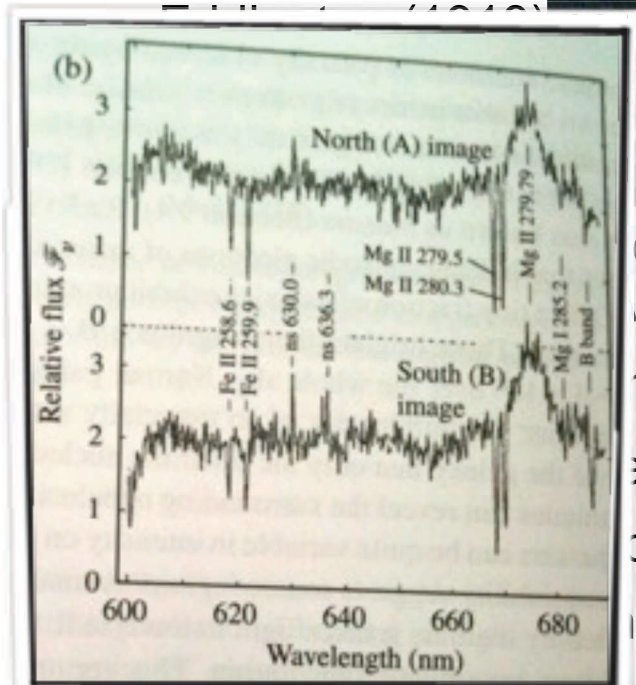
link to Newton and Laplace's formula

$$\alpha = \frac{2GM}{c^2} \frac{1}{r}$$

with r = (distance to Sun)

near the solar limb

of "fictitious stars" of different geometry



considers the same possibility (also rings) and concludes there is no net effect for stellar-mass lenses..

this new galaxy mass estimates ($\sim 4 \times 10^{11} M_{\odot}$) concluded:

lenses can split images to large observable angles

used to estimate galaxy masses

can lead to access distant faint galaxies!

- Kaiser (1984): time delay from variability of multiple sources can be used to measure H_0 (if an accurate mass model is available..)
- Walsh et al. (1979) discover lensed QSO0957+561 (6" apart)

Brief historical perspective

- Hypothesis
- Laplace
- Einstein
- a faint
- Eddington
- Chwolson
- star
- Einstein
- little
- Zwicky

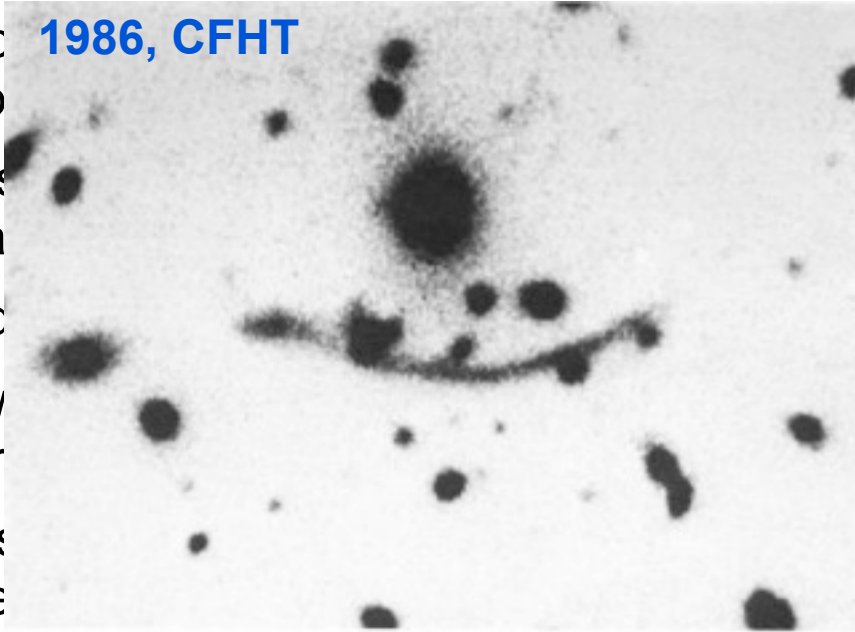
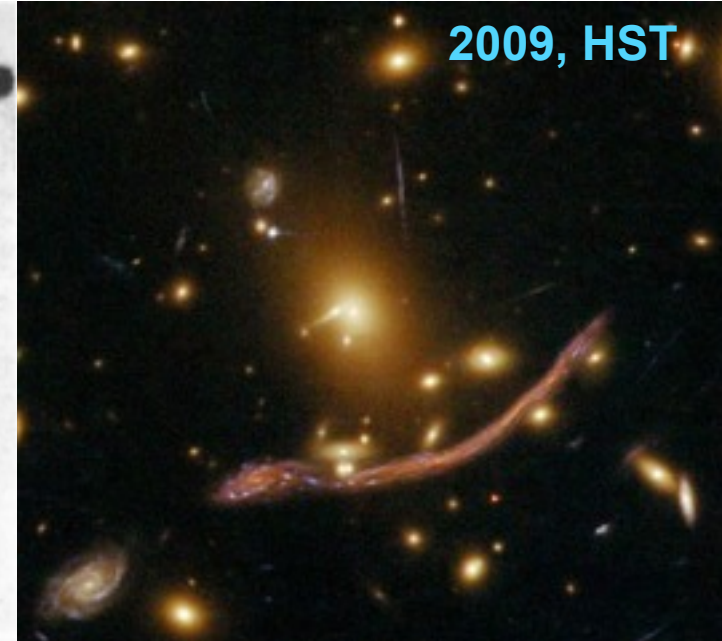


Figure 2: The giant luminous arc in Abell 370. CFHT, 0'2/pixel, 10 min., seeing 0'7, November 25, 1986.



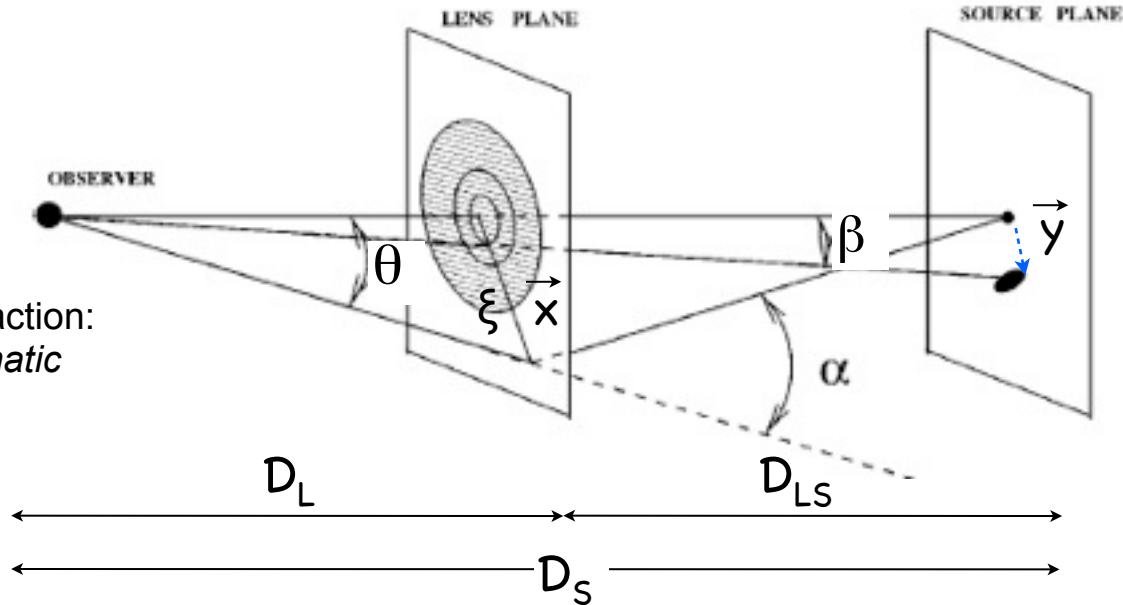
$$\alpha = \frac{2GM}{c^2 r}$$

limb
 (stars") of
 here is

- Zwicky estimates ($\sim 4 \times 11 M_{\odot}$) concluded:
 - lensing by galaxies can split images to large observable angles
 - this could be used to estimate galaxy masses
 - magnification can lead to access distant faint galaxies!
- Refsdal (1964): time delay from variability of multiple sources can be used to measure H_0 (if an accurate mass model is available..)
- Walsh et al. (1979) discover lensed QSO0957+561 (6" apart)
- First giant arcs discovered (Soucail et al. 87). Paczynski (87): right interpretation

Lensing Equation

- weak field approx:
 $\Phi = GM/r \ll c^2$
- thin lens approx
- effective index of refraction:
 $n = 1 - 2\Phi/c^2 \Rightarrow$ achromatic



$$\alpha = \frac{4GM}{c^2} \frac{1}{r}$$

point-mass element
for the mass element

- A lens is fully characterized by its surface mass density $\Sigma(\theta)$, or $K(\theta) = \Sigma(\theta)/\Sigma_{\text{crit}}$ (convergence), $\Sigma_{\text{crit}} = c^2/(4\pi G) \cdot D_S/(D_{LS}D_L)$

- Lensing mapping: $\beta = \theta - D_{LS}/D_S \alpha(\theta)$, where

$$\vec{\alpha}(\vec{\xi}) = \frac{4G}{c^2} \int \frac{(\vec{\xi} - \vec{\xi}') \Sigma(\vec{\xi}')}{|\vec{\xi} - \vec{\xi}'|^2} d^2\xi'$$

deflection angle

$$\begin{aligned} x &= \theta D_L \\ y &= \beta D_L \end{aligned}$$

$$\text{or: } \mathbf{y} = \mathbf{x} - \mathbf{D} \left(\frac{\Omega_M \Omega_\Lambda z_L z_S}{D_{LS} D_L} \right) \cdot \nabla \psi(\mathbf{x})$$

$$\uparrow$$

$$(D_{LS} D_L)/D_S$$

$$\uparrow$$

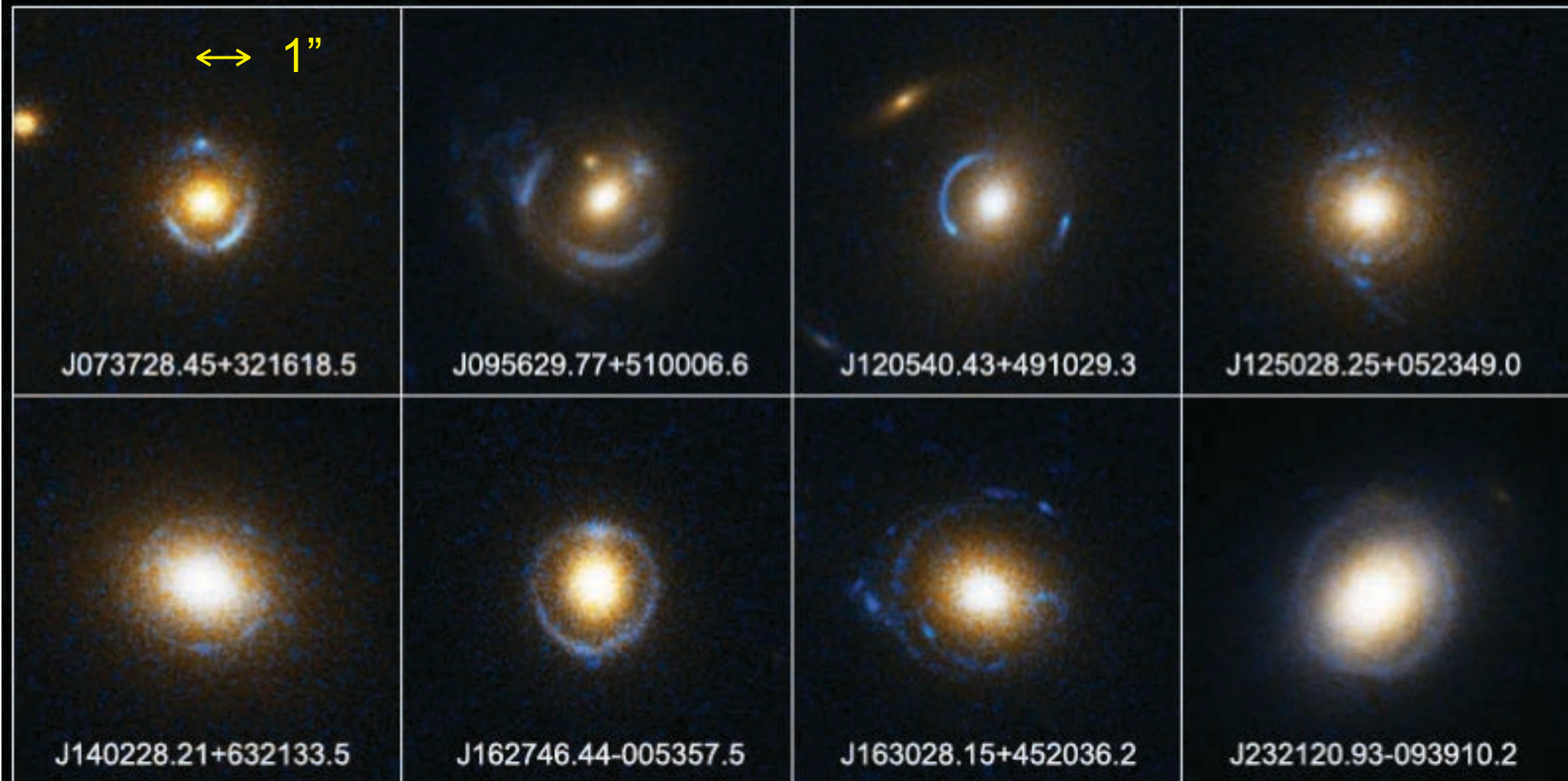
deflection potential = $1/\pi \int K(\mathbf{x}) \log|\mathbf{x} - \mathbf{x}'| d^2\mathbf{x}'$

- For circularly symmetric (supercritical) lens with a mass profile $M(\theta)$, a source on the optical axis ($\beta=0$) is imaged as ring with radius θ_E :

$$\beta(\theta) = \theta - \frac{D_{ds}}{D_d D_s} \frac{4GM(\theta)}{c^2 \theta} \quad \theta_E = \left[\frac{4GM(\theta_E)}{c^2} \frac{D_{ds}}{D_d D_s} \right]^{1/2} = \begin{cases} (0.9 \text{ mas}) \left(\frac{M}{M_\odot} \right)^{1/2} \left(\frac{D}{10 \text{ kpc}} \right)^{-1/2} \\ (0.9) \left(\frac{M}{10^{11} M_\odot} \right)^{1/2} \left(\frac{D}{\text{Gpc}} \right)^{-1/2} \end{cases}$$

Einstein Ring Gravitational Lenses

Hubble Space Telescope ■ ACS

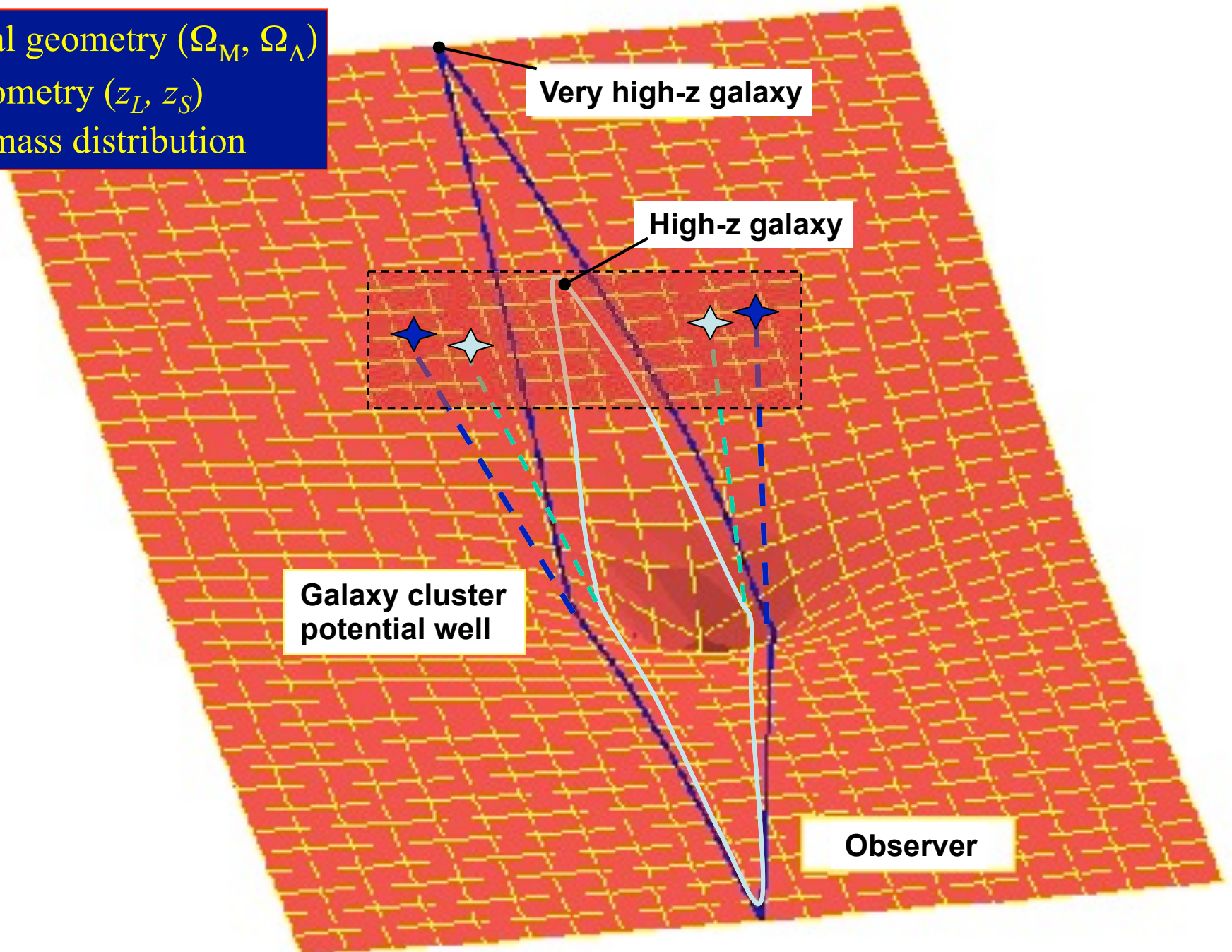


NASA, ESA, A. Bolton (Harvard-Smithsonian CfA), and the SLACS Team

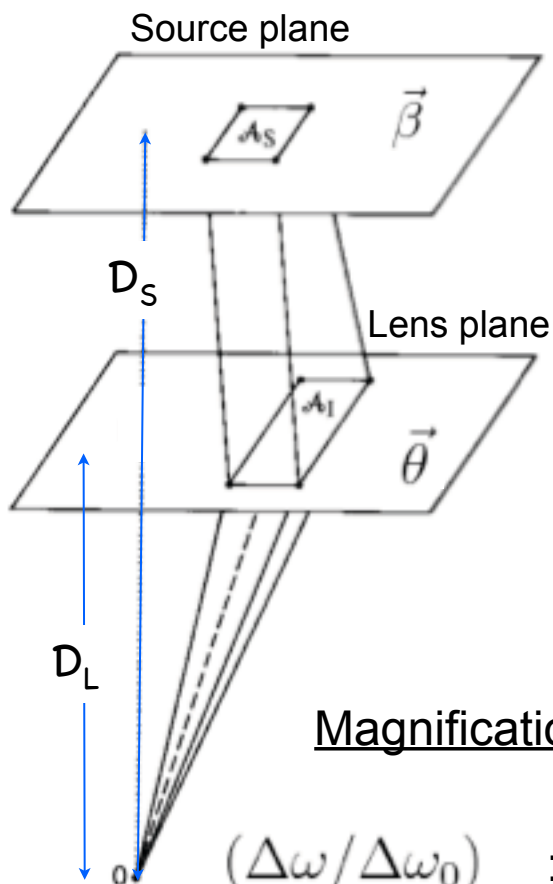
STScI-PRC05-32

Lensing mapping: $\mathbf{y} = \mathbf{x} - \mathbf{D}(\Omega_M, \Omega_\Lambda, z_L, z_S) \cdot \nabla \psi(\mathbf{x})$

- Universal geometry (Ω_M, Ω_Λ)
- Lens geometry (z_L, z_S)
- Cluster mass distribution



Magnification and image distortion



Light beams are subject to differential deflection (in this example the image of the source is magnified)

$$\Delta\omega_S = A_S/D_S^2 \quad \text{undeflected source solid angle}$$

$$\Delta\omega = A_I/D_L^2 \quad \text{observed image solid angle}$$

$$\text{Observed flux: } S_\nu = I_\nu \Delta\omega$$

Surface brightness, I_ν , does not change (both per unit freq. and integrated).

Flux of the image

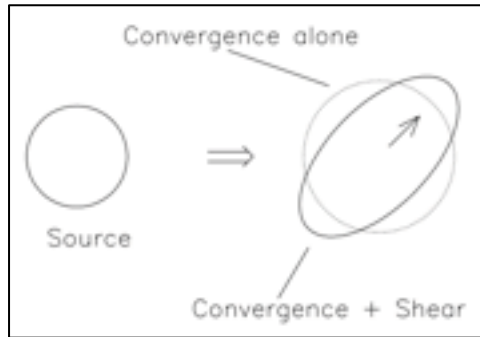
Magnification: $\mu = S_I/S_0 = \left(\frac{\Delta\omega}{\Delta\omega_0} \right)$ is frequency independent (S_0 : flux of unlensed source)

$(\Delta\omega/\Delta\omega_0)$: area distortion of the lens mapping $\vec{\theta} \rightarrow \vec{\beta}$
 given by $\vec{\beta} = \vec{\theta} - \vec{\alpha}(\vec{\theta})$

$$\Delta\omega_0 = \left| \frac{\partial(\beta_1, \beta_2)}{\partial(\theta_1, \theta_2)} \right| \Delta\omega \equiv \left| \frac{\partial\vec{\beta}}{\partial\vec{\theta}} \right| \Delta\omega$$

$$\left| \frac{\partial\vec{\beta}}{\partial\vec{\theta}} \right| \equiv \text{Jacobian}_{\vec{\beta} \rightarrow \vec{\theta}} \equiv \det \left(\frac{\partial\vec{\beta}}{\partial\vec{\theta}} \right) \quad A_{ij} = \partial\beta_i/\partial\theta_j$$

Convergence and Shear



convergence magnifies the image isotropically, the *shear* deforms it to an ellipse (anisotropic part of the lens mapping, i.e. “astigmatism”)

$$\vec{\alpha}(\vec{\theta}) = \vec{\nabla}\psi = \frac{1}{\pi} \int \kappa(\vec{\theta}') \frac{\vec{\theta} - \vec{\theta}'}{|\vec{\theta} - \vec{\theta}'|^2} d^2\theta'$$

Locally, the lens mapping is described by the Jacobian matrix \mathcal{A} : $\vec{\beta} = \vec{\theta} - \vec{\alpha}(\vec{\theta})$

$$\mathcal{A} \equiv \frac{\partial \vec{\beta}}{\partial \vec{\theta}} = \left(\delta_{ij} - \frac{\partial \alpha_i(\vec{\theta})}{\partial \theta_j} \right) = \left(\delta_{ij} - \frac{\partial^2 \psi(\vec{\theta})}{\partial \theta_i \partial \theta_j} \right) = \mathcal{M}^{-1} \quad (\text{inverse of the magnification tensor})$$

Magnification is the ratio of the solid angles of the image and the source:

$$\frac{\delta\theta^2}{\delta\beta^2} = \det \mathcal{M} = \frac{1}{\det \mathcal{A}} \quad \frac{\partial^2 \psi}{\partial \theta_i \partial \theta_j} \equiv \psi_{ij} \quad (\text{derivatives of the lensing potential})$$

The lensing effect can be decomposed into a *shear* tensor:

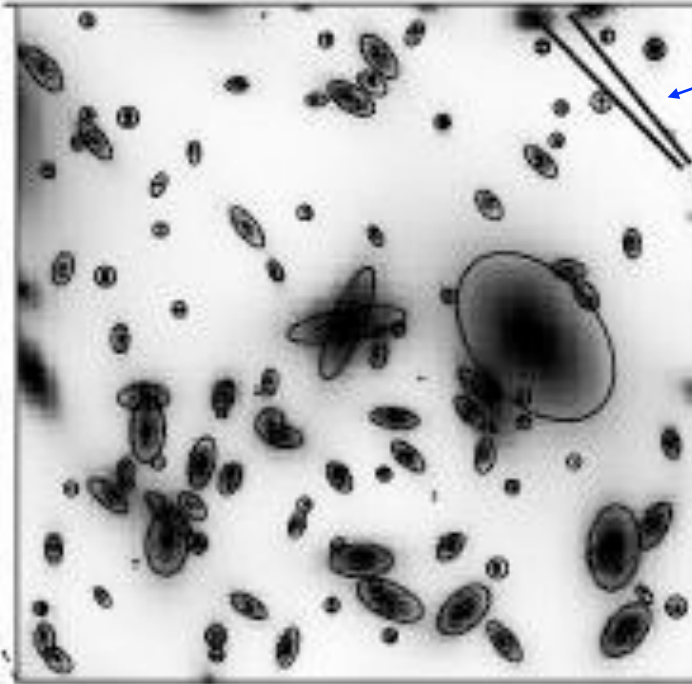
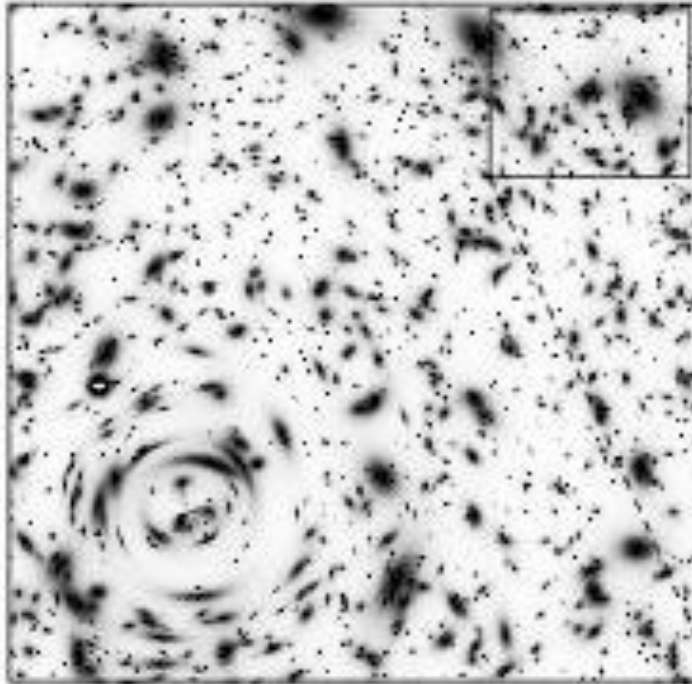
$$\begin{aligned} \gamma_1(\vec{\theta}) &= \frac{1}{2} (\psi_{11} - \psi_{22}) \equiv \gamma(\vec{\theta}) \cos [2\phi(\vec{\theta})], & \gamma &= (\gamma_1^2 + \gamma_2^2)^{1/2} \text{ is the magnitude of the shear} \\ \gamma_2(\vec{\theta}) &= \psi_{12} = \psi_{21} \equiv \gamma(\vec{\theta}) \sin [2\phi(\vec{\theta})]. & \phi & \text{ the orientation} \end{aligned}$$

and an isotropic term (*convergence*): $\kappa = \frac{1}{2} (\psi_{11} + \psi_{22}) = \frac{1}{2} \text{tr} \psi_{ij}$ $\rightarrow \mathcal{A} = \begin{pmatrix} 1 - \kappa - \gamma_1 & -\gamma_2 \\ -\gamma_2 & 1 - \kappa + \gamma_1 \end{pmatrix}$

Under the transformation $\vec{\beta} = \mathcal{A} \vec{\theta}$, a circular object gains an ellipticity $(a-b)/(a+b)$ of:

$$\mathcal{g} = \gamma / (1 - \kappa) \quad (\text{reduced shear}), \text{ with magnification: } \mu = \det \mathcal{M} = \frac{1}{\det \mathcal{A}} = \frac{1}{[(1 - \kappa)^2 - \gamma^2]}$$

Strong and Weak lensing from a cluster with projected surface mass density $K(\theta)$



Avg orientation
of gals yields
the "shear"

$$K(\theta) = \Sigma(\theta) / \Sigma_{\text{cr}}$$

$$\Sigma_{\text{cr}} = \frac{c^2 D_s}{4\pi G D_d D_{ds}}$$

Strong lensing regime:

$$K(\theta) \gtrsim 1$$

Giant arcs, multiple images.

By iterating the mapping

$\beta \leftrightarrow \vartheta$ of multiple images with

known redshift one can invert

the lensing equation, i.e.

determine the deflection field

Weak lensing regime:

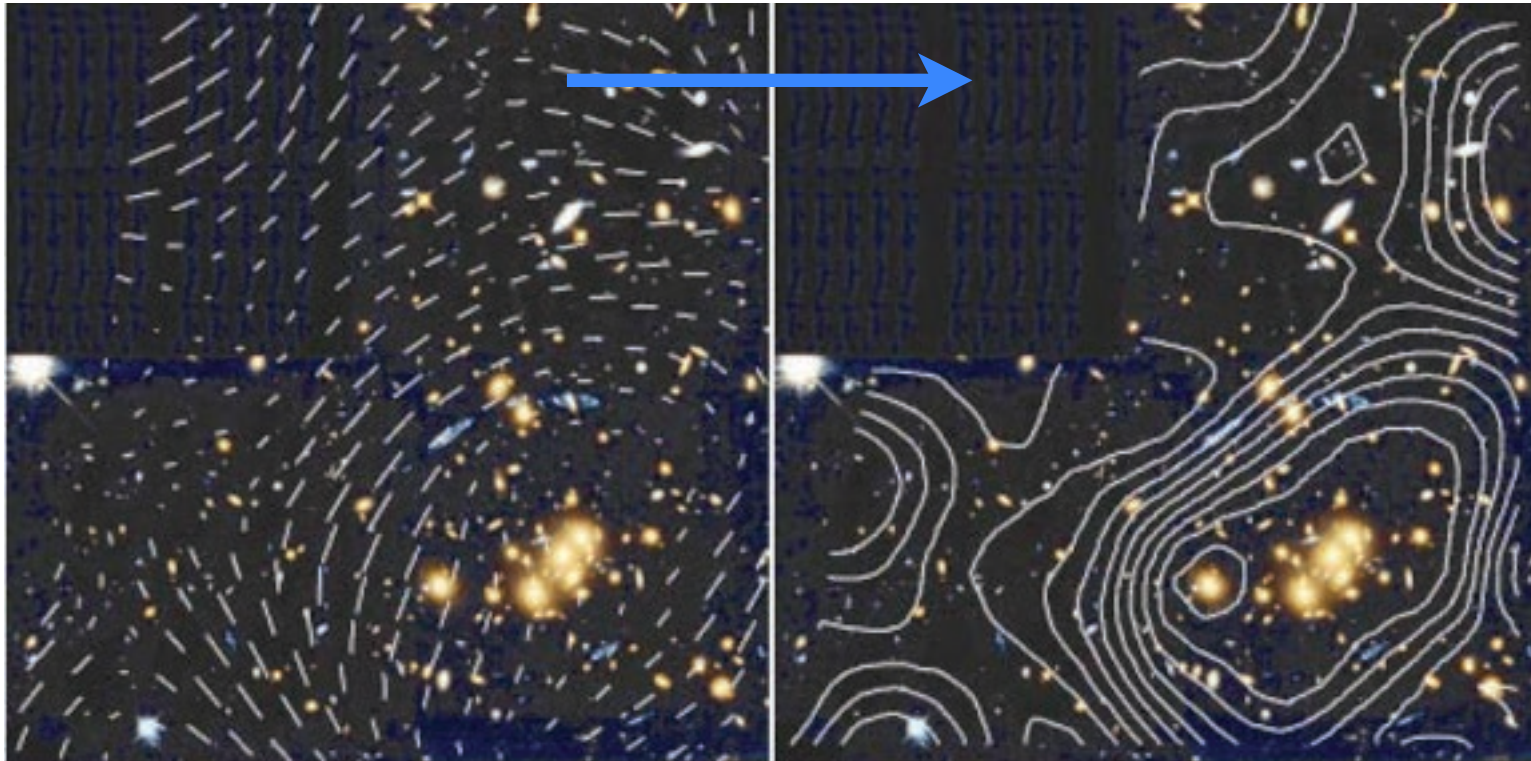
$$K(\theta) \ll 1$$

From the statistical distortion of
background galaxy shapes (averaged
ellipticities) \rightarrow reduced shear

(once corrected for the PSF).

If the redshift distribution of the
sources is known the mass distribution
can be inverted up to a constant

From shear to mass...



- shape measurements to provide ellipticities of background galaxies (requires selection of background), need to average over several background galaxies
→ resolution limit to mass reconstruction
- correct for seeing and PSF distortions or other instrumental effects (e.g. CTE)
- convert measured ellipticities to a surface density map $\kappa(\vartheta)$ using KS method
- surface mass density is obtained from $\Sigma(\vartheta) = \kappa(\vartheta) \times \Sigma_{\text{crit}}(D_L, D_S, D_{LS})$
 - requires a knowledge of background redshift distribution!

From shear to mass...

Mass-sheet degeneracy:

Any reconstruction method is insensitive to isotropic expansions of images

→ the measured ellipticities are invariant against replacing \mathcal{A} with $\lambda \mathcal{A}$

$$\mathcal{A}' = \lambda \mathcal{A} = \lambda \begin{pmatrix} 1 - \kappa - \gamma_1 & -\gamma_2 \\ -\gamma_2 & 1 - \kappa + \gamma_1 \end{pmatrix}$$

which is equivalent to leaving the reduced shear g invariant under the transformation: $(\kappa \rightarrow 1 - \lambda + \lambda\kappa)$

Possible solutions:

- Fix κ somewhere on the image:
 - assume that the shear is zero at edge of the image
 - use a model (e.g. NFW) to fit the κ profile

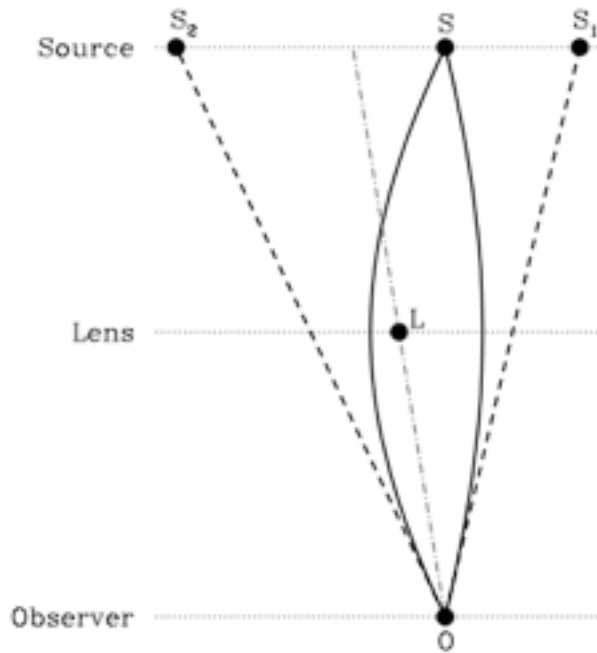
- Use SL data (e.g. multiple images)

- Measure independently the magnification since $\mu = \frac{1}{(1 - k)^2 - \gamma^2} \propto \lambda^{-2}$

“magnification bias”, or number counts depletion (Broadhurst et al.):

$$N'(m) = N_0(m) \mu^{2.5s-1} \quad s = \frac{d \log N(m)}{dm}$$

Time delay and H_0



$$(\vec{\theta} - \vec{\beta}) - \vec{\nabla}_{\theta} \psi = 0,$$

lens equation

or

$$\vec{\nabla}_{\theta} \left(\frac{1}{2} (\vec{\theta} - \vec{\beta})^2 - \psi \right) = 0.$$

↑ “Fermat” potential $\phi(\theta, \beta)$

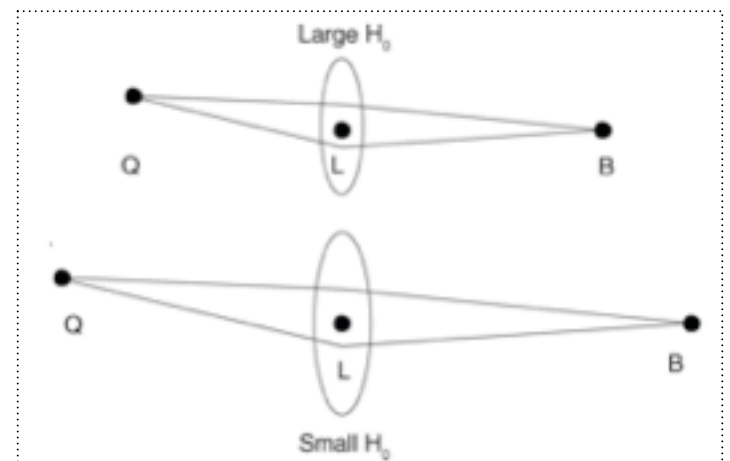
$$\tau(\vec{\theta}, \vec{\beta}) = \tau_{\text{geom}} + \tau_{\text{grav}} = \frac{1 + z_L}{c} \frac{D_L D_S}{D_{LS}} \left(\frac{1}{2} (\vec{\theta} - \vec{\beta})^2 - \psi(\theta) \right).$$

Masses bend passing light similarly to convex lenses.

Fermat’s principle in gravitational lensing optics for a medium with an index of refraction $n = 1 - \frac{2\Phi}{c^2}$

Images occur where the τ is extremal, i.e. $\vec{\nabla}_{\theta} \tau = 0$.

Time delay $\sim H_0^{-1} \rightarrow$ if a robust model is available for the lensing potential, $\psi(\theta)$, then by monitoring the time delay of variable sources (QSOs) H_0 can be measured in one step.



Singular Isothermal Sphere (SIS) and non-singular Isothermal Ellipsoid (NIE)

- Simple model for mass distribution of galaxies assuming stars as self-gravitating ideal gas of particles in “thermal equilibrium” ($T \sim \sigma_v^2 = \text{const}$)

$$\boxed{\rho(r) = \frac{\sigma_v^2}{2\pi G} \frac{1}{r^2}} \quad v_{\text{rot}}^2(r) = \frac{GM(r)}{r} = 2\sigma_v^2 = \text{constant} \quad (\text{flat rotation curves in galaxies})$$

Surface mass density: $\Sigma(\xi) = \frac{\sigma_v^2}{2G} \frac{1}{\xi} \quad \theta_E = 4\pi \frac{\sigma_v^2}{c^2} \frac{D_{ds}}{D_s} = 1.4'' \left(\frac{\sigma_v}{220 \text{ km/s}} \right)^2 \frac{D_{ds}}{D_s}$

$$\langle \Sigma(\theta_{\text{arc}}) \rangle \approx \langle \Sigma(\theta_E) \rangle = \Sigma_{\text{cr}} \quad (\text{for circular sym. lenses})$$

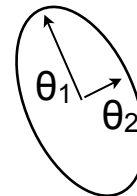
$$M(\theta) = \Sigma_{\text{cr}} \pi (D_d \theta)^2 \approx 1.1 \times 10^{14} M_{\odot} \left(\frac{\theta}{30''} \right)^2 \left(\frac{D}{1 \text{ Gpc}} \right)$$

- Tangential (giant) arcs constrain the *projected* mass density within the circle traced by the arcs

Softened IS with core (**NIS**): $r^2 \rightarrow r^2 + r_c^2 \quad \frac{1}{\xi} \rightarrow \frac{\xi}{(\xi^2 + \xi_c^2)^{1/2}}$

Generalization to **Elliptical lenses (NIE)**:

$$\Sigma(\theta_1, \theta_2) = \frac{\Sigma_0}{[\theta_c^2 + (1 - \varepsilon)\theta_1^2 + (1 + \varepsilon)\theta_2^2]^{1/2}}$$

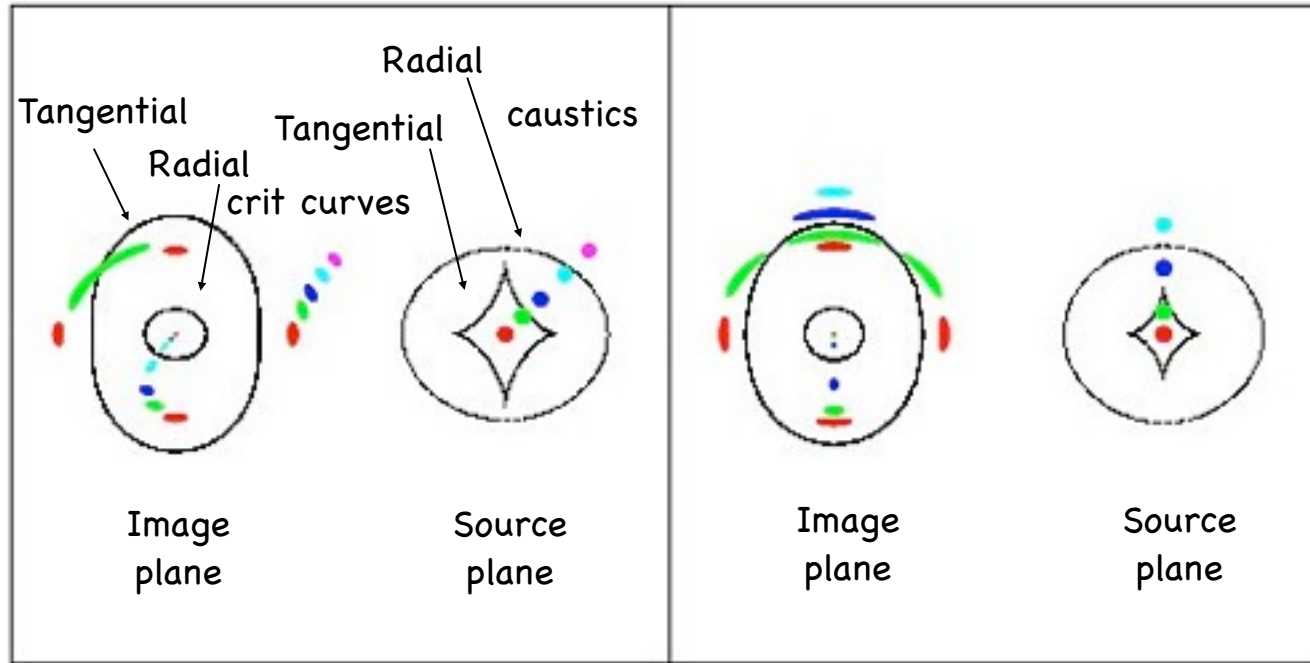


Strong lensing: basics optics

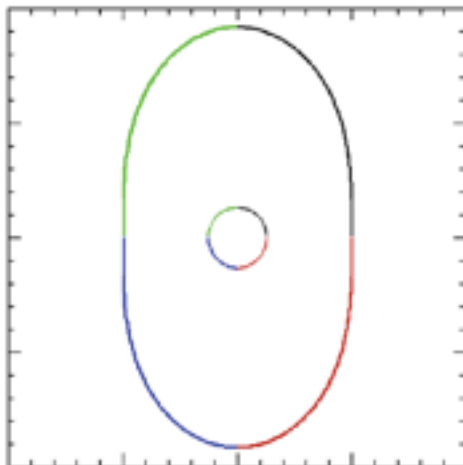
Elliptical lens: compact source crossing..

..a fold caustic

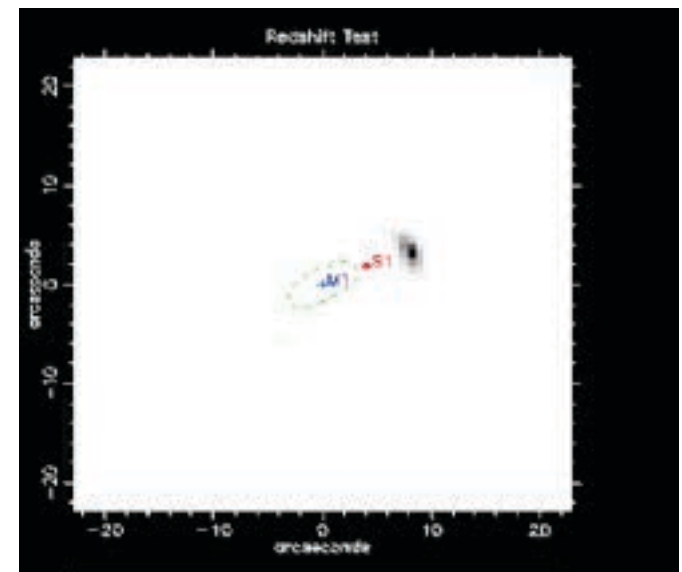
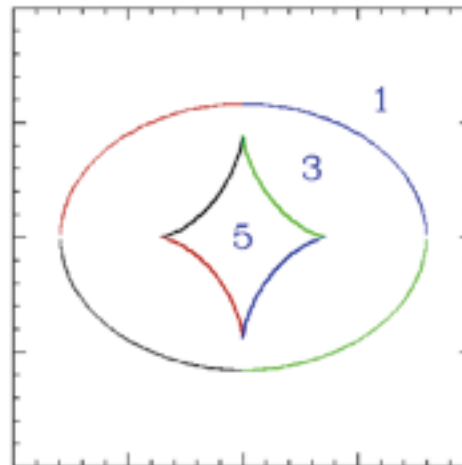
..a cusp caustic



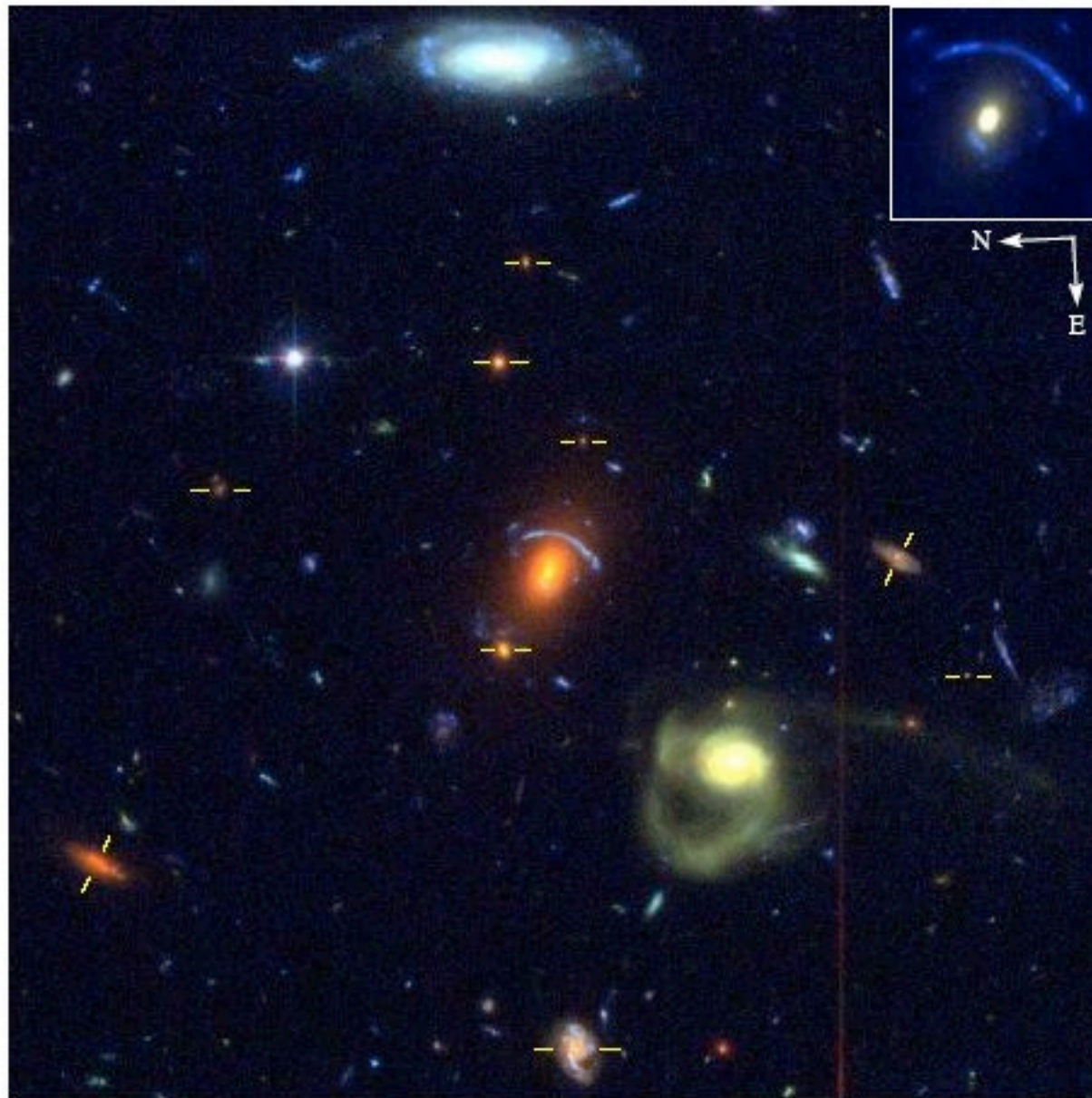
Critical curves



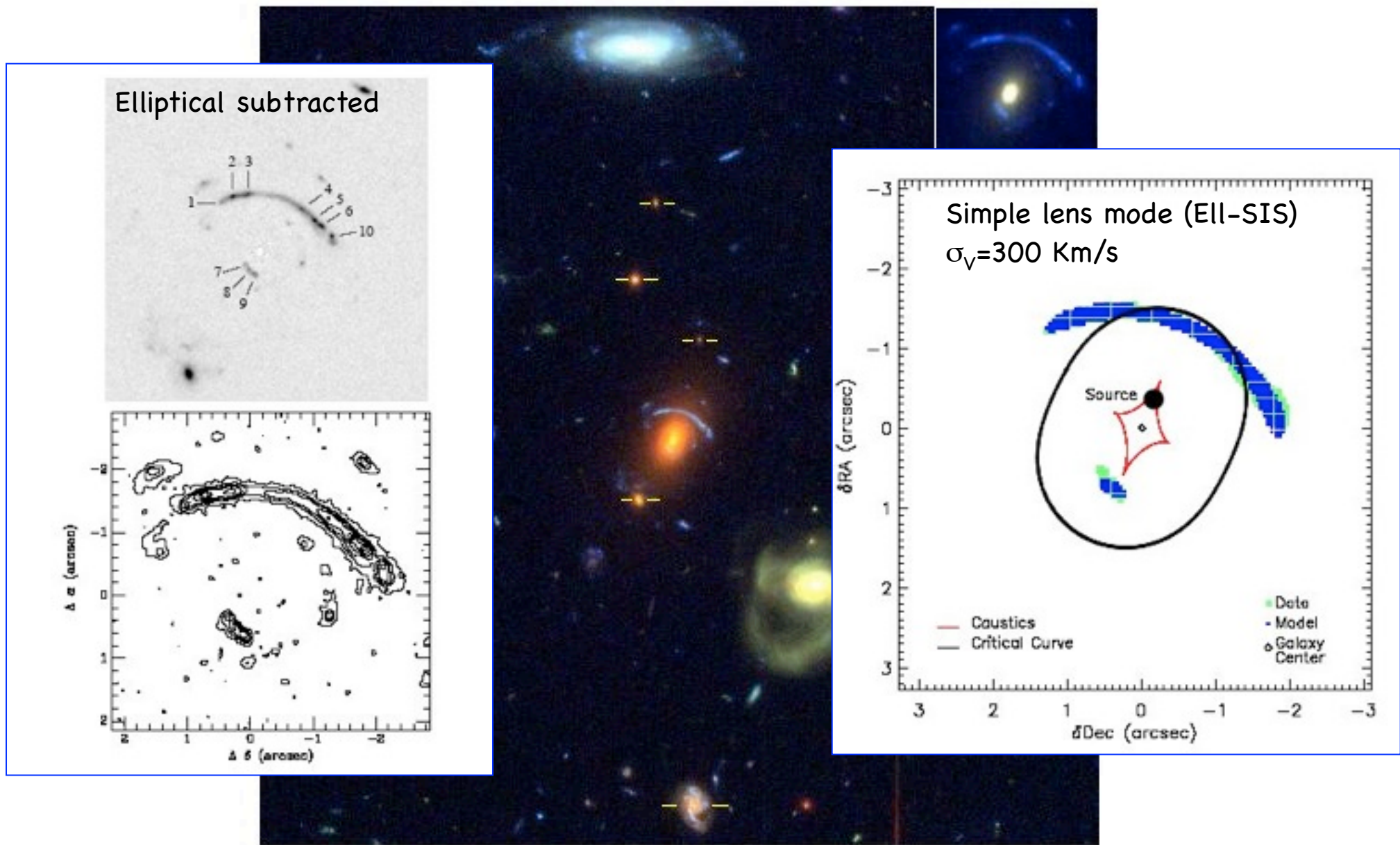
Caustics



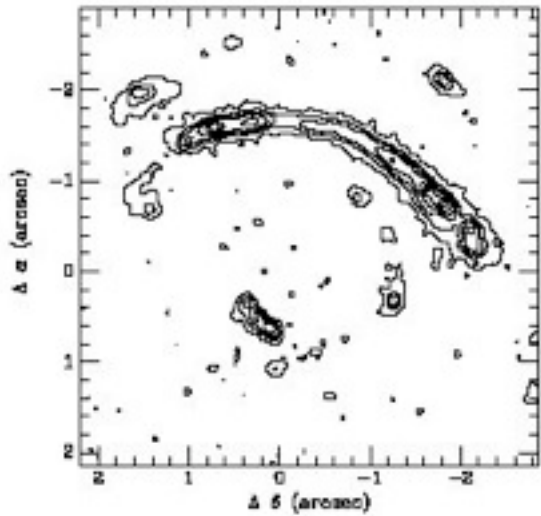
A serendipitous discovery: $z_L=0.62$, $z_S(\text{phot}) \approx 2.4$
in a deep HST/ACS field



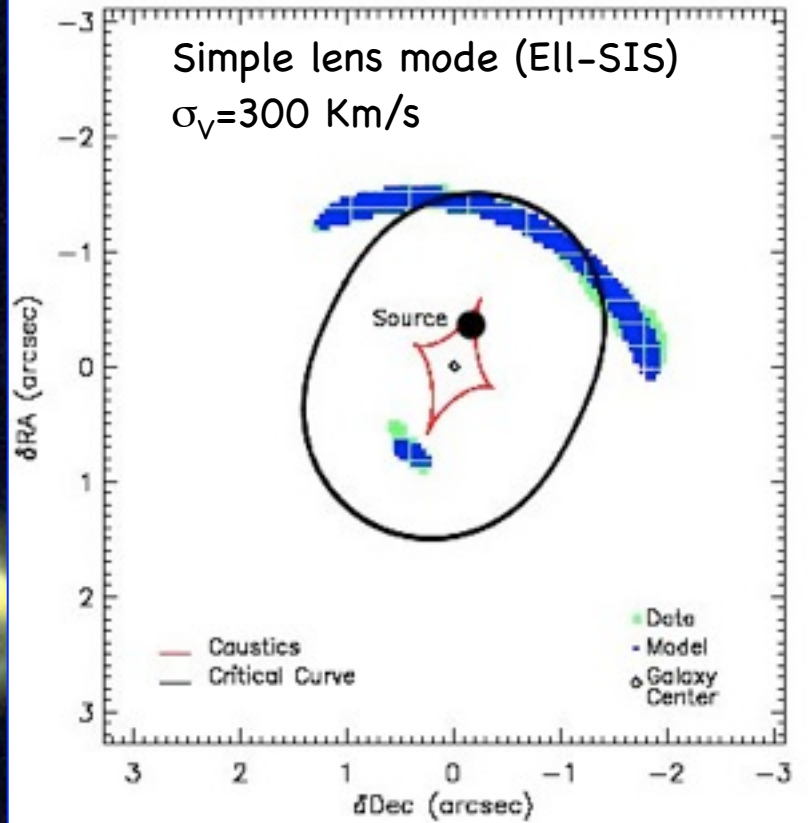
A serendipitous discovery: $z_L=0.62$, $z_S(\text{phot}) \approx 2.4$
in a deep HST/ACS field



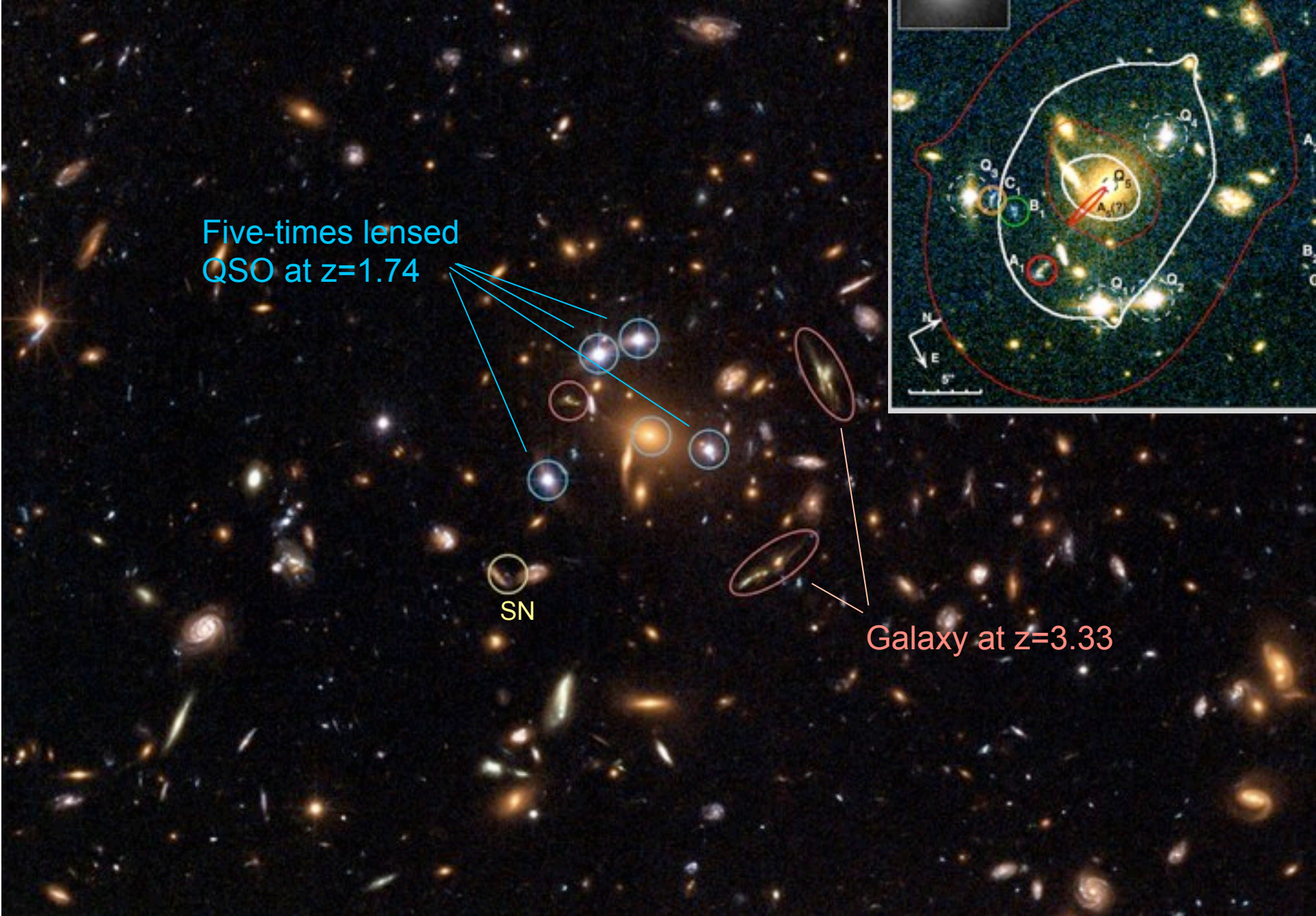
Elliptical subtracted



Simple lens mode (Ell-SIS)
 $\sigma_V=300$ Km/s

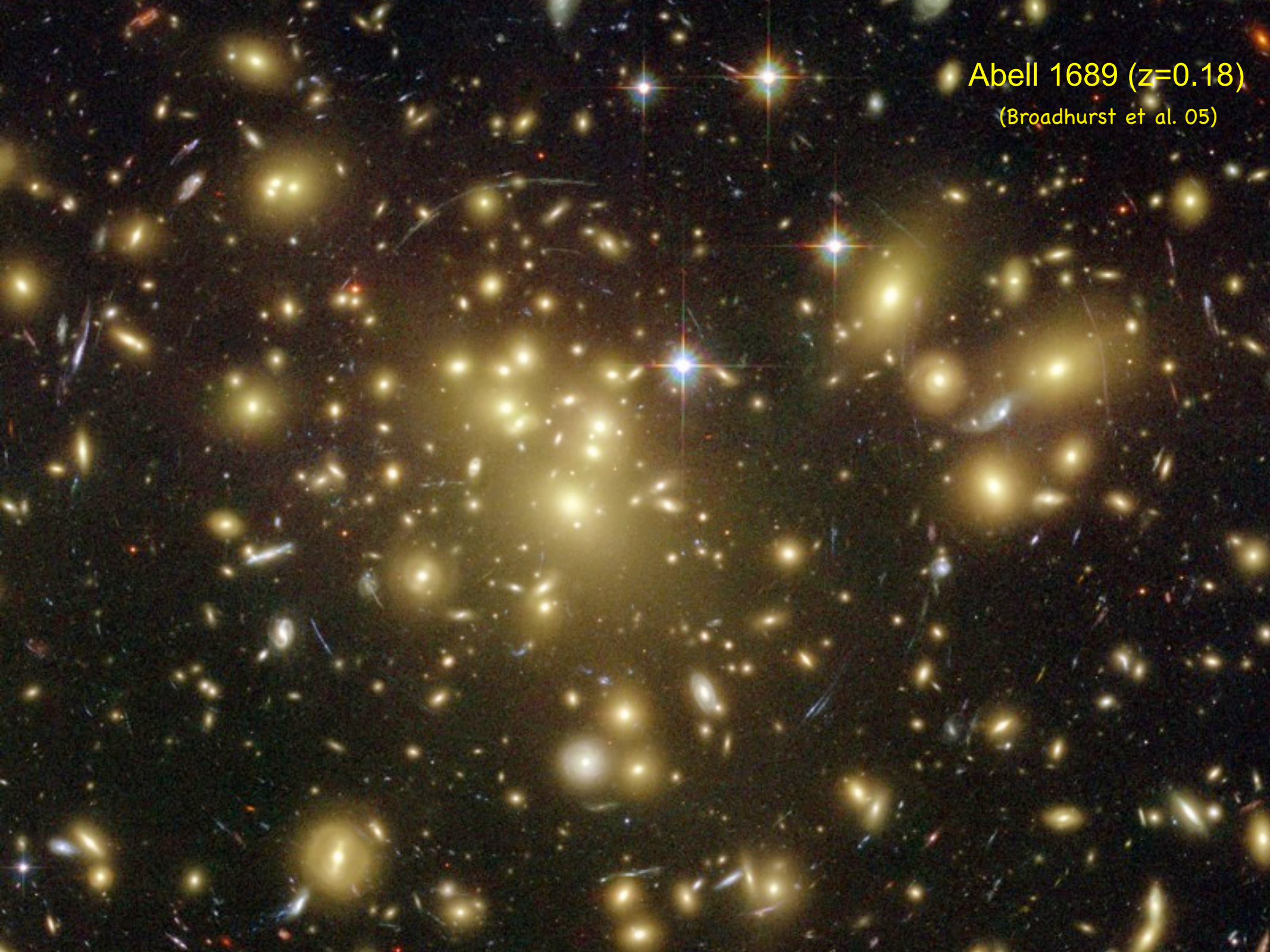


SDSS J1004+4112 ($z=0.68$)



Abell 1689 ($z=0.18$)

(Broadhurst et al. 05)



Best fit (projected) mass model (green contours)

from the identification of 106 multiple images of 30 independent sources!

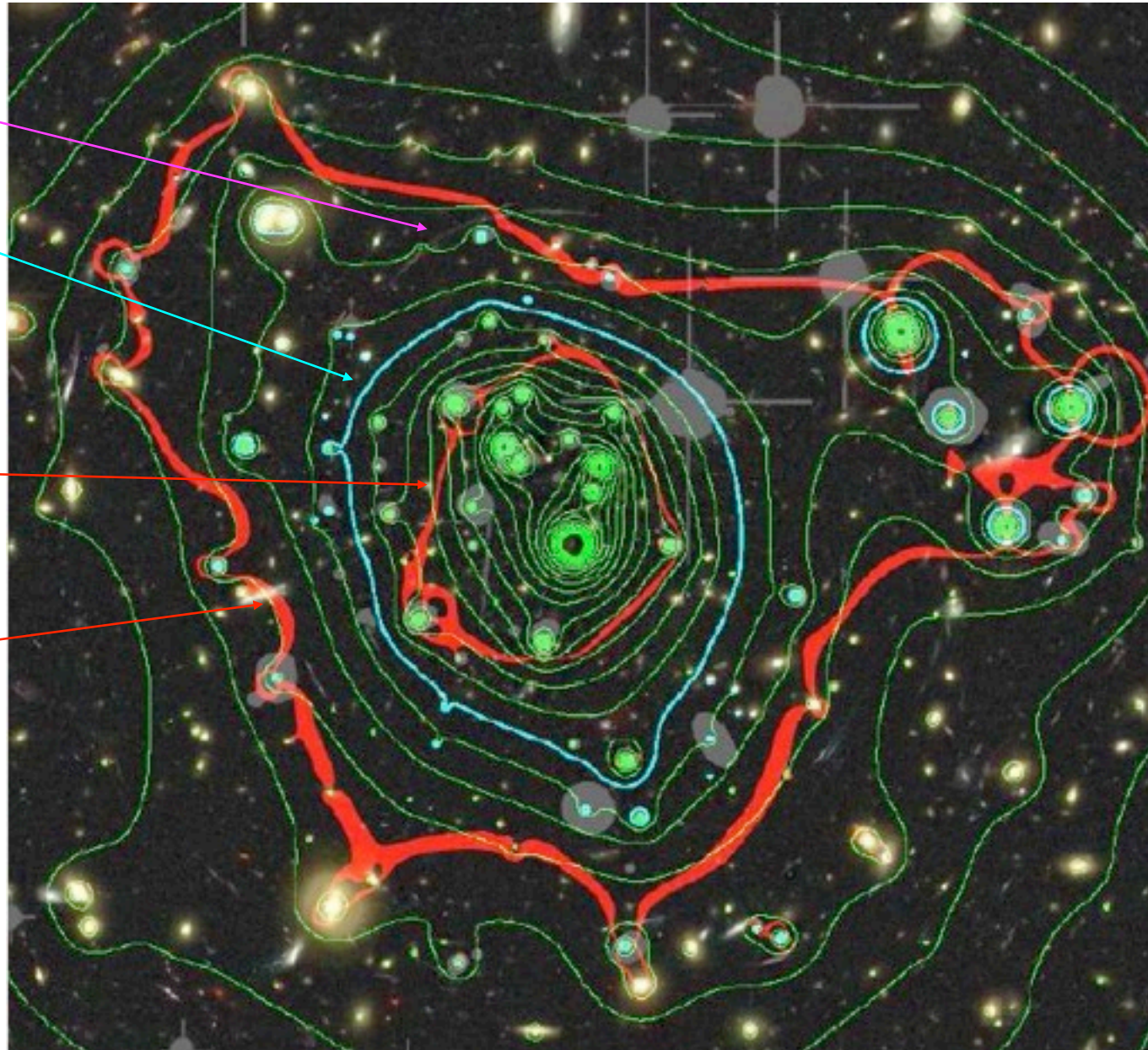
(Broadhurst et al. 05)

Giant arc bisected
by the critical curve

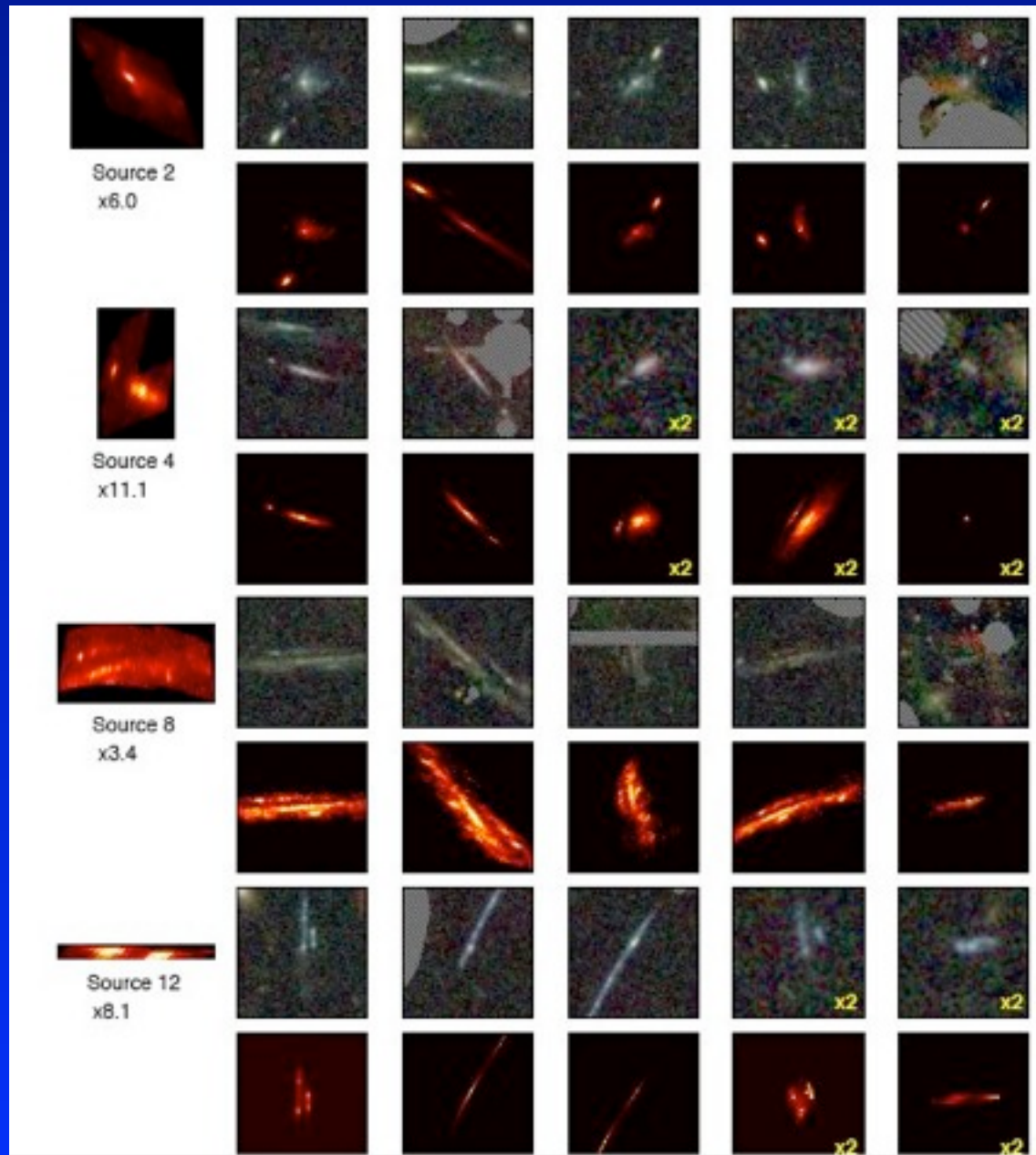
Critical surface
mass density
contour ($\Sigma = \Sigma_{\text{crit}}$)
scaled to $z=3$

Radial
critical
curve

Tangential
critical
curve



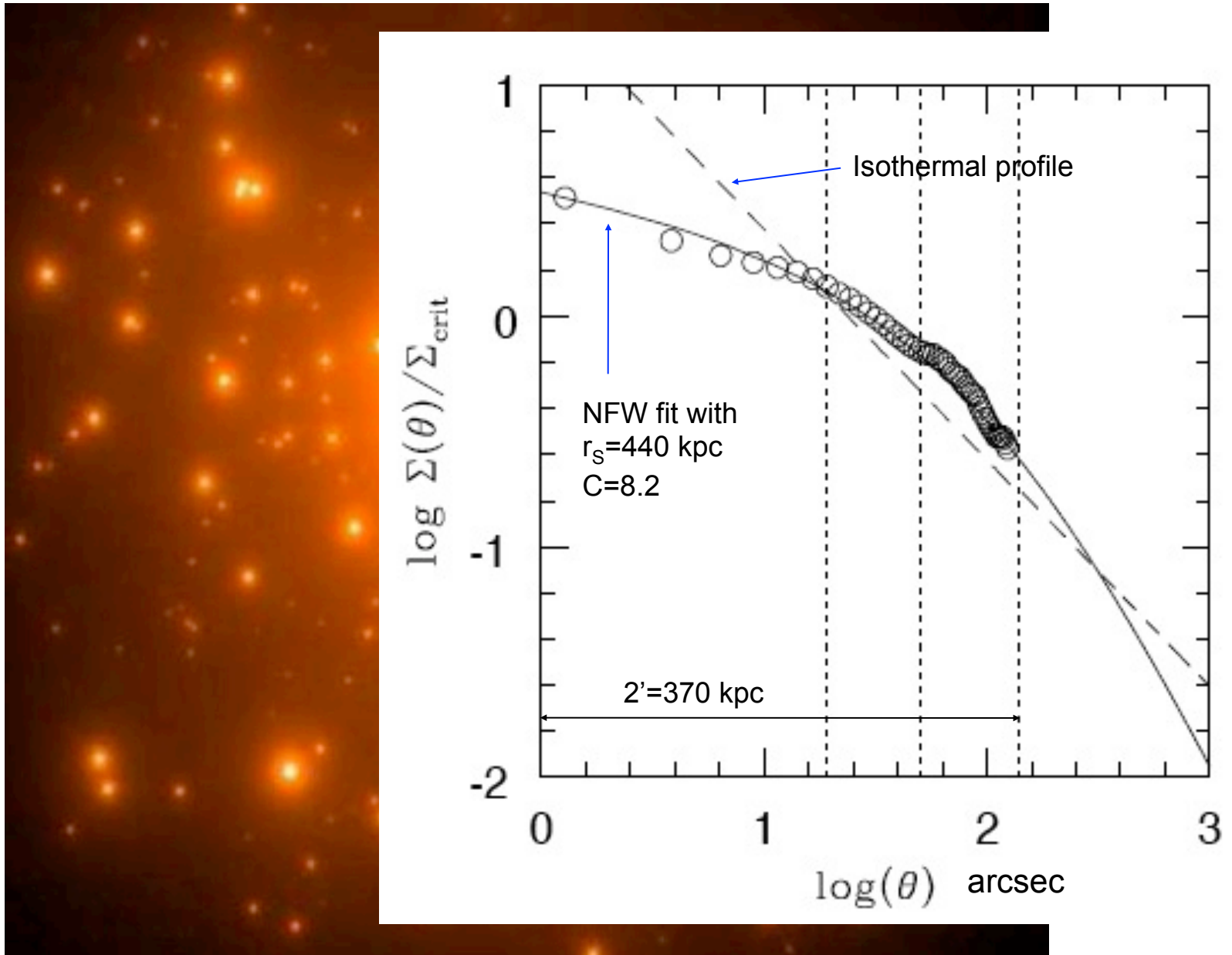
A gallery of multiple images in A1689...



Observed reconstructed mass map in A1689

(Broadhurst et al. 05)

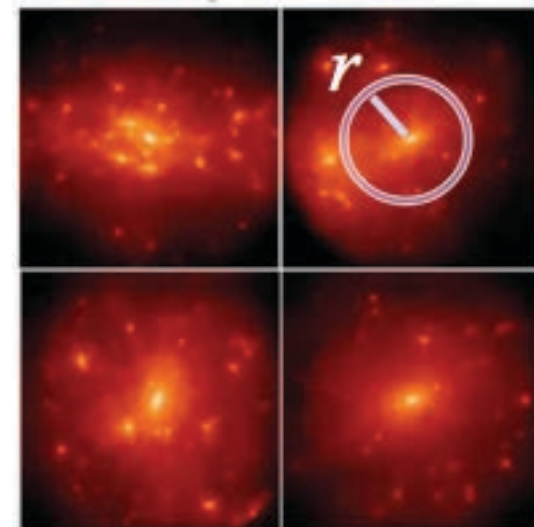




Theoretical NFW profile is found to be a good fit, albeit with much larger concentration than expected ($C \approx 4$ at these high masses)

Λ CDM Predictions for DM Mass Profiles

N-body simulations have shown (Navarro, Frenk, White 96, **NFW**) that CDM halos have self-similar profiles, differing only by simple rescaling of size and density over 4 decades in mass (gal \rightarrow CL)



Hierarchical assembly of CDM halos predicts:

1. mass profiles with a (quasi) universal shape
2. prominent triaxial shapes
3. “cuspy” inner mass slopes ($\beta \approx 1$)
4. a large degree of substructure

$$\rho(r) = \frac{\rho_s}{(r/r_s)(1 + r/r_s)^2}$$

concentration parameter

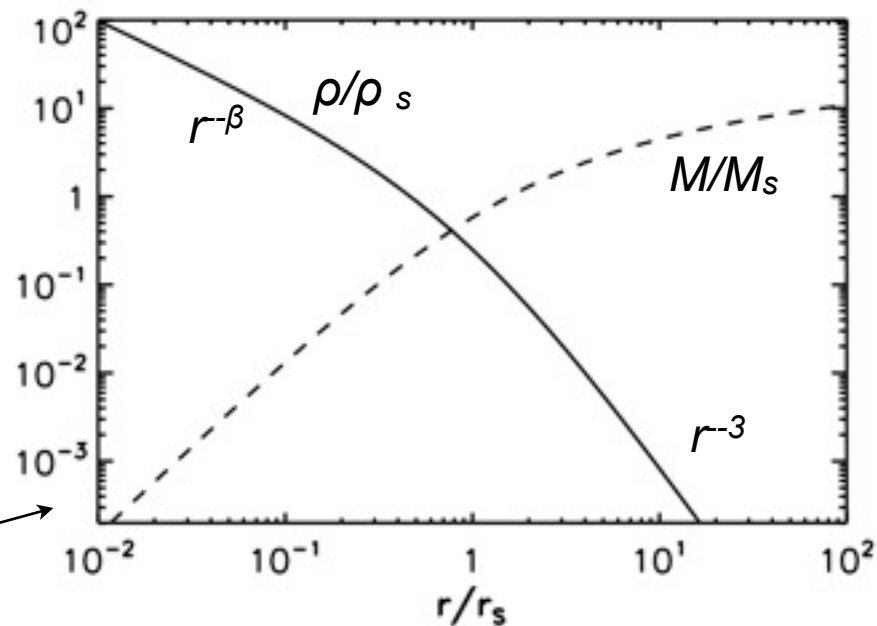
$$\bar{\rho} = 200\rho_{cr}(z) = \frac{3}{4\pi r_{200}^3} \int_0^{r_{200}} 4\pi r^2 dr \rho(r)$$

$$c \equiv \frac{r_{200}}{r_s}$$

$$\rho_s = \delta_c \rho_c, \quad \delta_c = (200/3)c^3 / [\ln(1+c) - c/(1+c)]$$

$$M(r) = 3M_s \left[\ln(1+x) - \frac{x}{1+x} \right], \quad x = r/r_s$$

gNFW
$$\rho(r) = \frac{\rho_s}{(r/r_s)^\beta (1 + r/r_s)^{(3-\beta)}}$$

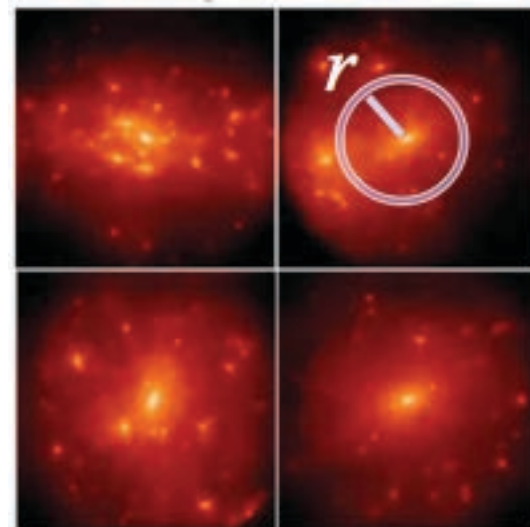


Λ CDM Predictions for DM Mass Profiles

N-body simulations have shown (Navarro, Frenk, White 96, **NFW**) that CDM halos have self-similar profiles, differing only by simple rescaling of size and density over 4 decades in mass (gal \rightarrow CL)

Hierarchical assembly of CDM halos predicts:

1. mass profiles with a (quasi) universal shape
2. prominent triaxial shapes
3. “cuspy” inner mass slopes ($\beta \approx 1$)
4. a large degree of substructure



$$\rho(r) = \frac{\rho_S}{(r/r_S)(1 + r/r_S)^2}$$

concentration parameter
 \downarrow

$$c \equiv \frac{r_{200}}{r_S}$$

$$\bar{\rho} = 200\rho_{cr}(z) = \frac{3}{4\pi r_{200}^3} \int_0^{r_{200}} 4\pi r^2 dr \rho(r)$$

$$\rho_S = \delta_c \rho_c, \quad \delta_c = (200/3)c^3 / [\ln(1+c) - c/(1+c)]$$

$$M(r) = 3M_S \left[\ln(1+x) - \frac{x}{1+x} \right], \quad x = r/r_S$$

$$\text{gNFW} \quad \rho(r) = \frac{\rho_S}{(r/r_S)^\beta (1 + r/r_S)^{(3-\beta)}}$$

Einasto profile

$$\rho_E(r) = \rho_S \exp \left[\frac{2}{\alpha} (1 - x^\alpha) \right], \quad x \equiv r/r_S$$

\uparrow
 $\rho_E(r_S)$

$$d \ln \rho_E / d \ln r = -2x^\alpha$$

ΛCDM Predictions for DM Halos (dependence of concentration on Redshift and Mass)

- Lensing studies have focused on constraining the inner slope β and concentration c with controversial results. Most data indicate shallow ($\beta < 1$) or cored ($\beta = 0$) inner regions, several studies indicate high concentrations
- Even if gravity is scale free, the halo concentration c_{vir} will depend on mass & redshift via the **formation epoch of DM halos** (env density of the Universe), which depends on the structure formation scenario

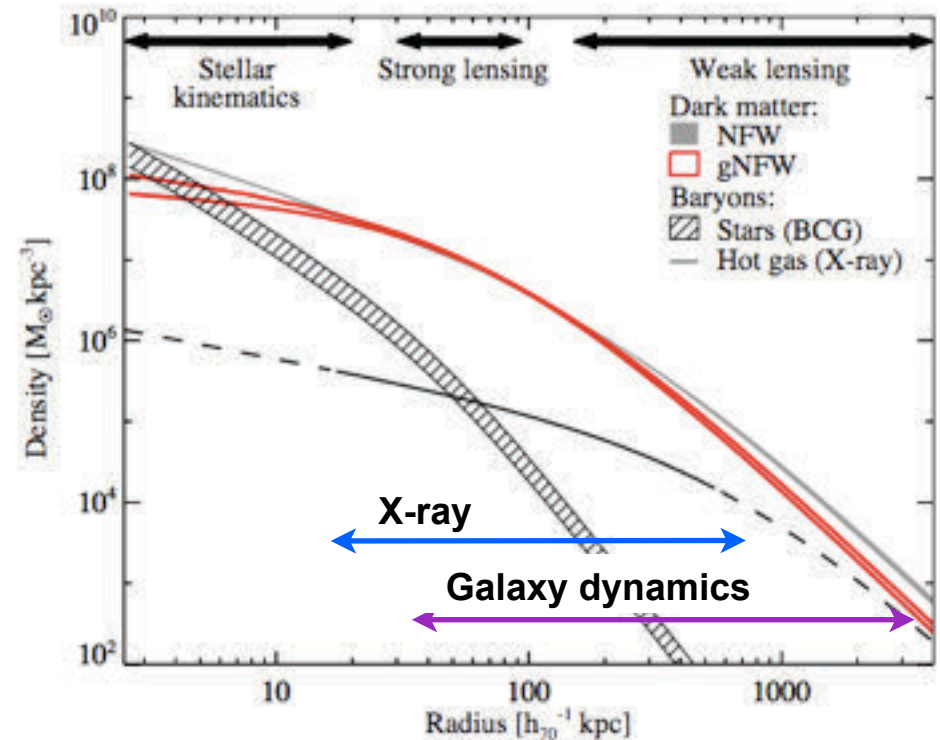
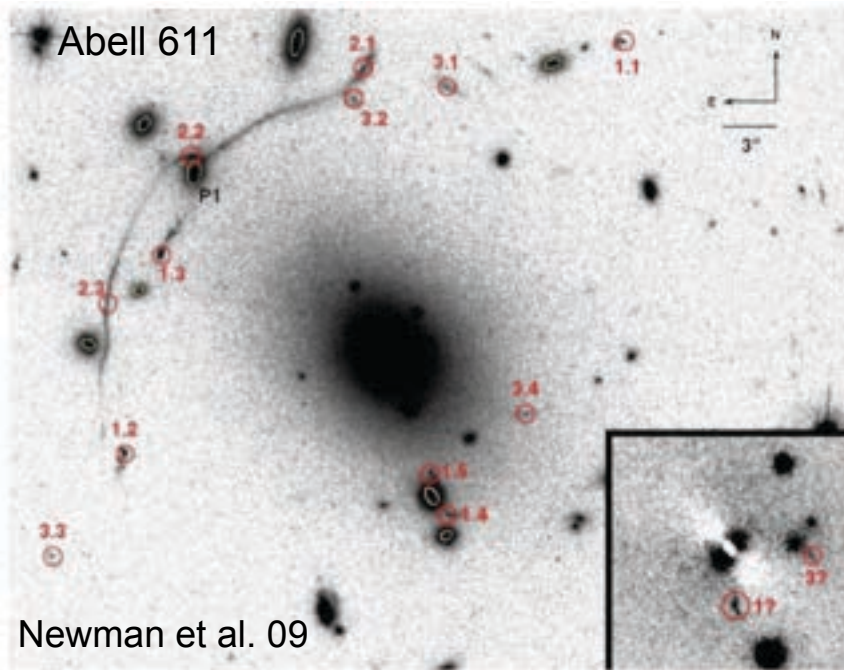
$$c_{vir} \equiv r_{vir}(M_{vir}, z) / r_s(z_{vir}) \quad \bar{c}_{vir} \approx c_0 (1+z)^{-A} \left(\frac{M_{vir}}{10^{15} M_{sun} / h} \right)^{-B} \quad \text{Duffy et al. 08}$$

Simulations suggest $A \approx 0.1$, $B \approx 0.7-1$, $c \approx 5$ (Log M=14-15)

- Massive objects formed later in ΛCDM, so massive objects have lower concentration
- $r_s(z_{vir})$ depends on structure formation, esp. formation epoch of progenitor; the characteristic overdensity

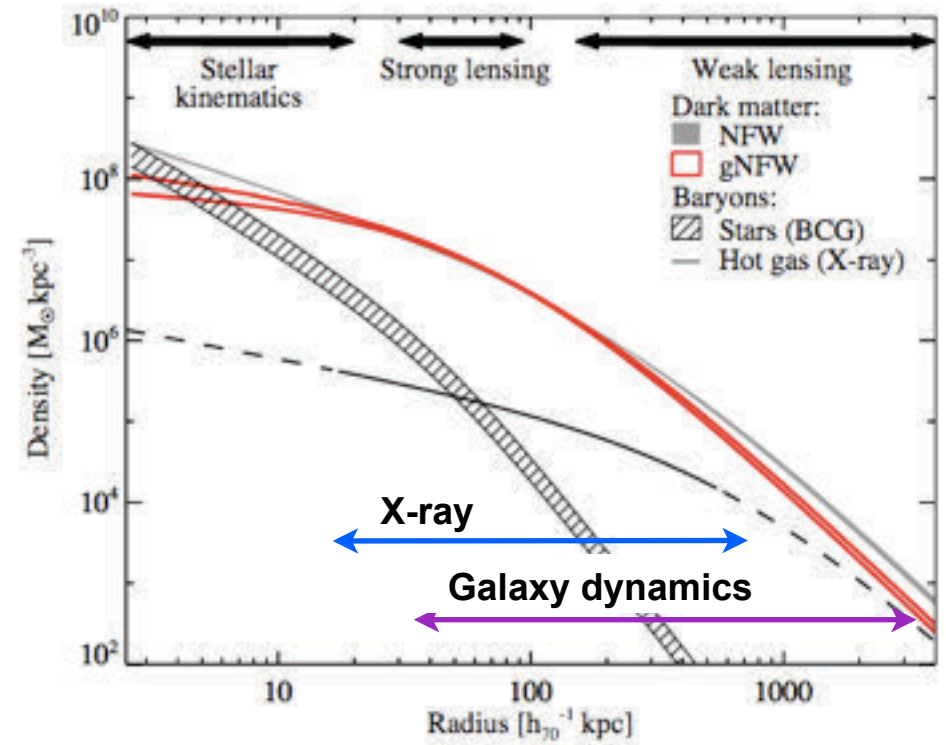
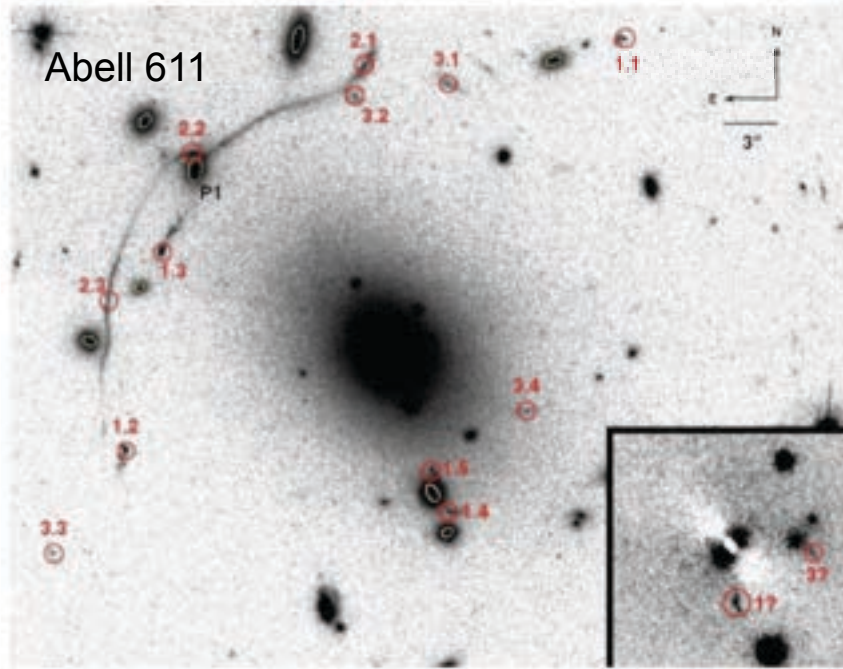
$$\delta_c \propto \Omega_M (1 + z_F)^3$$

DM mass distribution within clusters and the foundations of Λ CDM

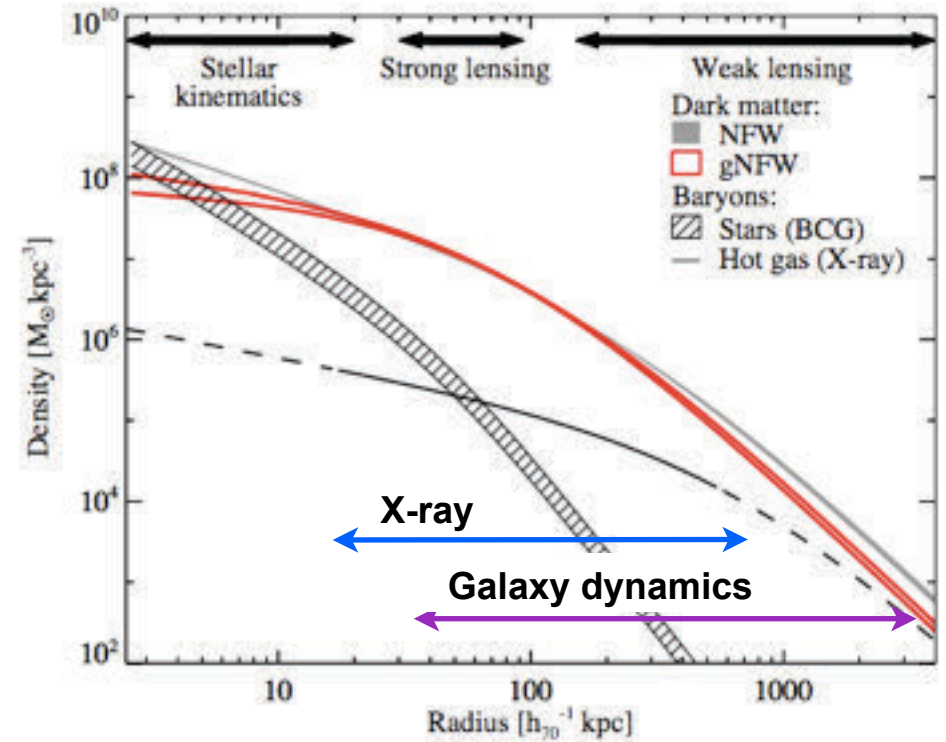
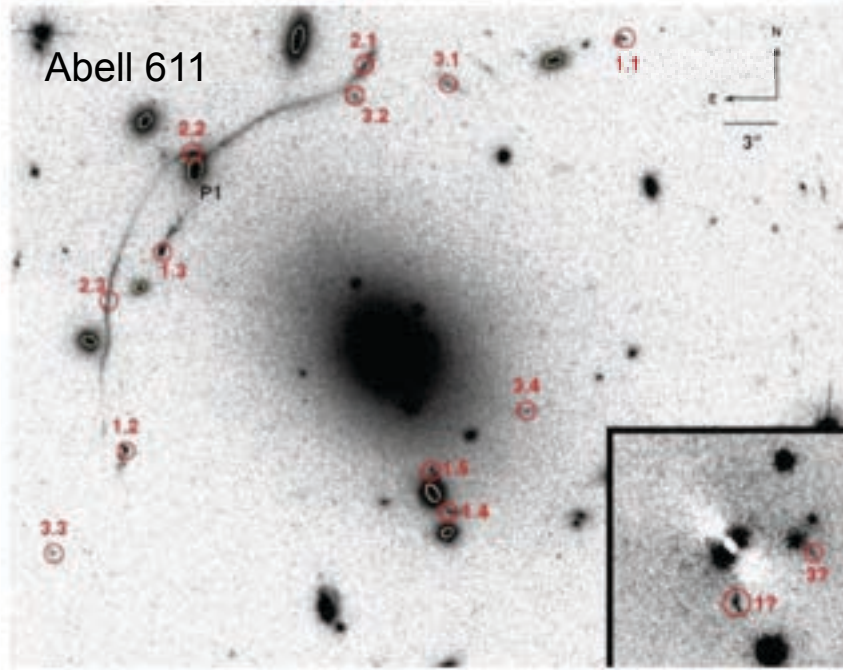


- Accurate mass density profiles of massive clusters can directly test Λ CDM scenario over ~ 30 -1000 kpc scales:
 - Test NFW predictions on DM concentration/slopes as a fnc of Mass and Redshifts
- Strong Lensing: unique probe of inner DM profile \rightarrow can constrain DM properties
- Key: use a variety of complementary probes covering 2-3 decades in scale, degeneracies (inner slope, concentration and M^*/L) are mitigated

DM and Baryon mass density profiles in clusters

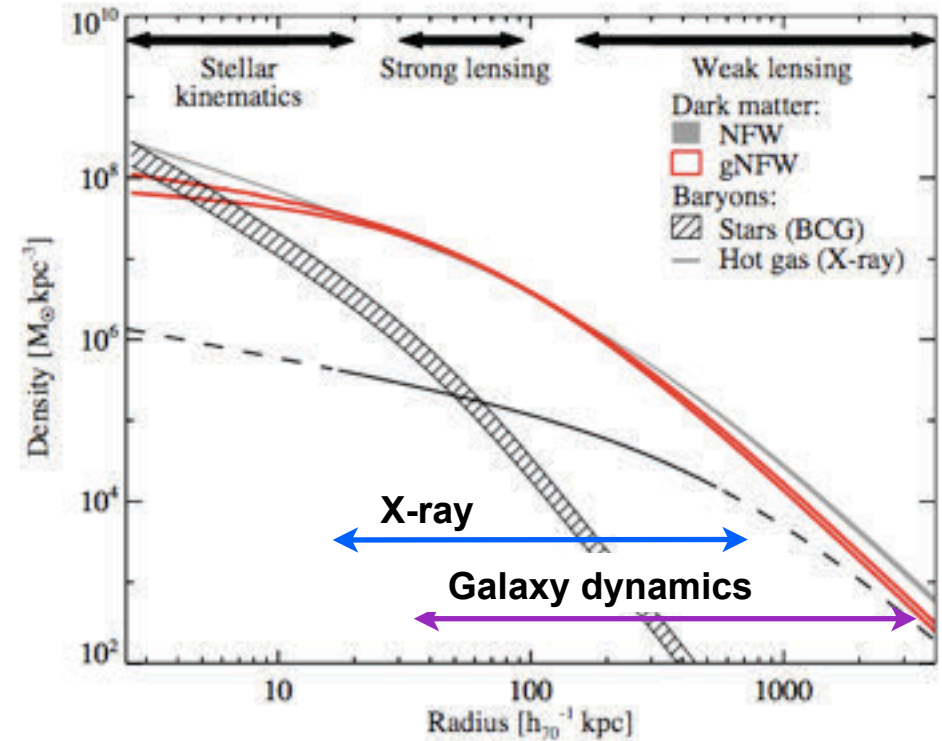
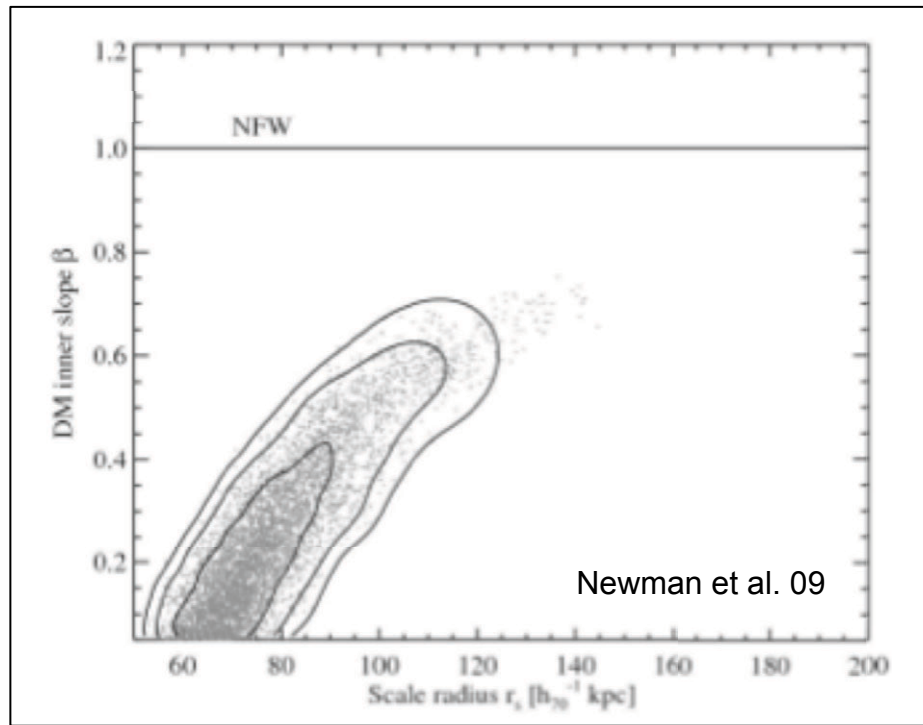


DM and Baryon mass density profiles in clusters



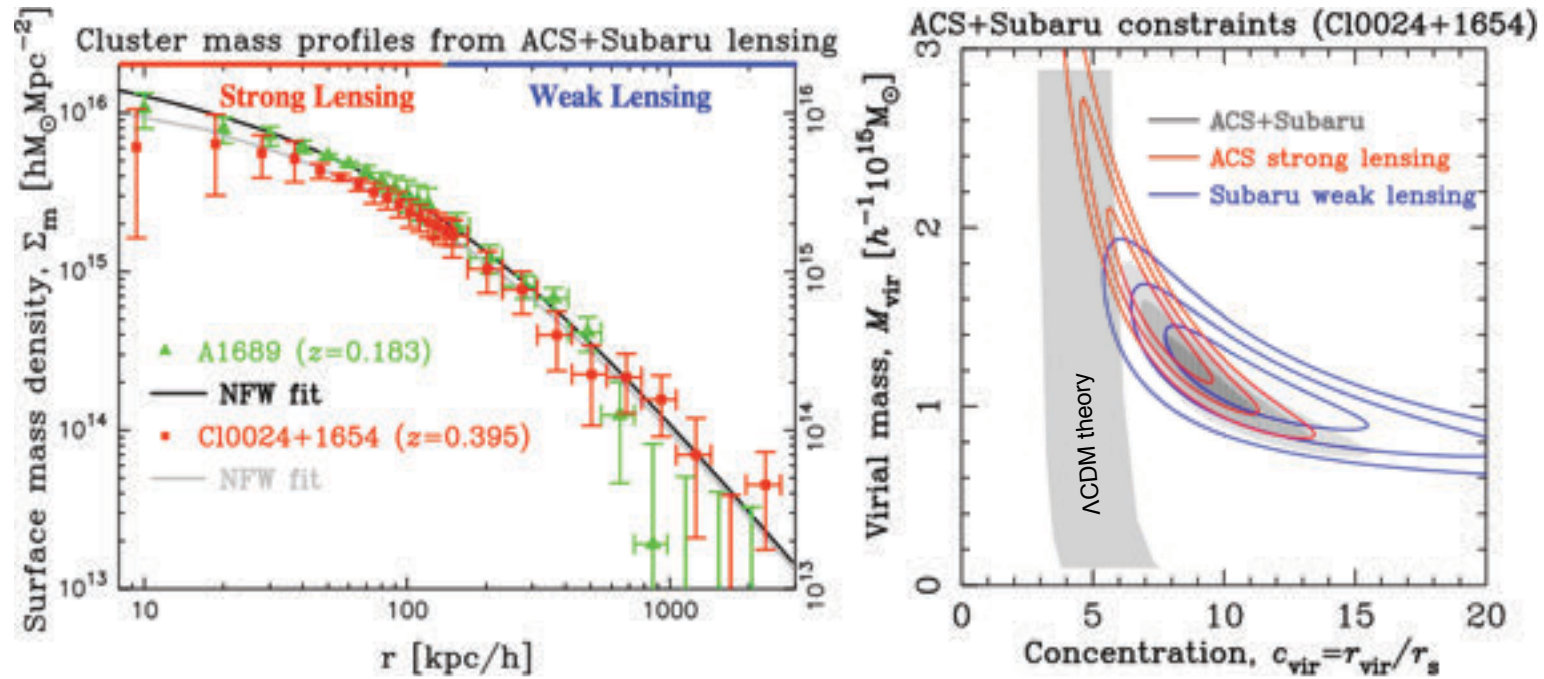
- Early results point to a *possible* tension with Λ CDM:
shallow inner slopes, large mass concentrations, large Einstein radii:

DM and Baryon mass density profiles in clusters



- Early results point to a *possible* tension with Λ CDM:
shallow inner slopes, large mass concentrations, large Einstein radii:

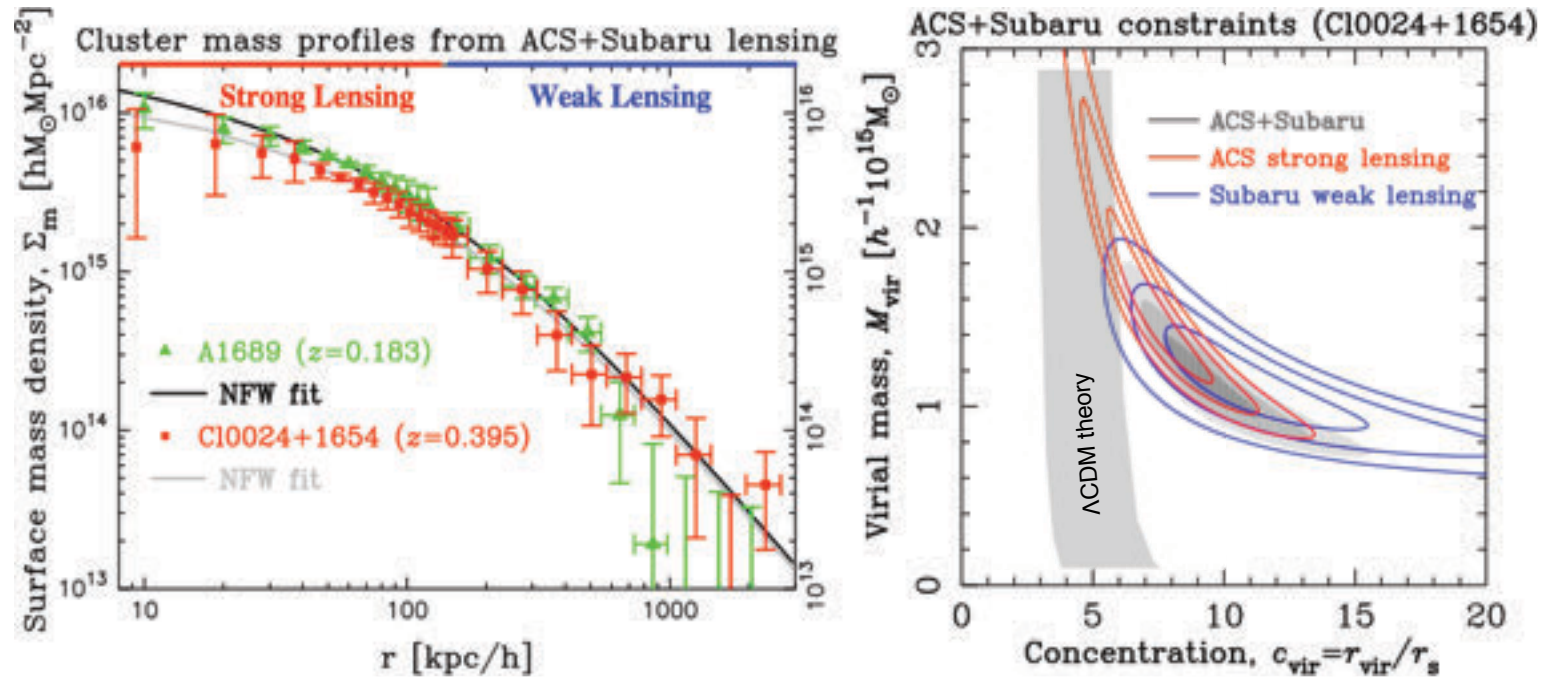
DM and Baryon mass density profiles in clusters



Umetsu&Broadhurst 2008

- Early results point to a *possible* tension with Λ CDM:
shallow inner slopes, large mass concentrations, large Einstein radii:

DM and Baryon mass density profiles in clusters



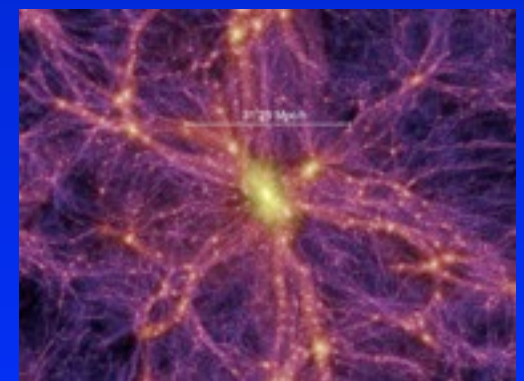
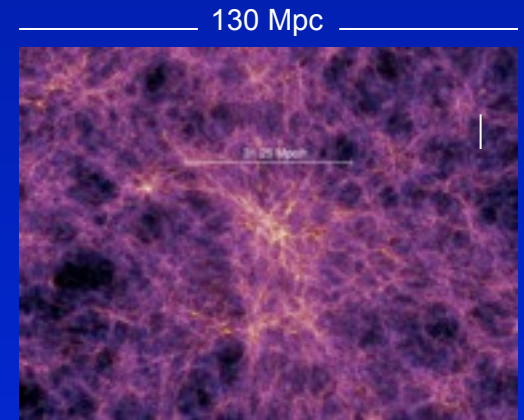
Umetsu&Broadhurst 2008

- Early results point to a *possible* tension with ΛCDM :
shallow inner slopes, large mass concentrations, large Einstein radii:
 - ▶ Formation of clusters at earlier times than expected? non-gauss. fluctuations?
 - ▶ Does ΛCDM have problems on small scales despite the success on large scales?
 - ▶ Do we understand how baryonic physics shapes the inner DM potential?
 - ▶ Is DM really collision-less?
- *But this is based on a handful of clusters..* small (biased) samples? triaxiality? cl-cl variance?

Cluster masses and inner structure of DM halos

Fundamental Questions that Remain Unanswered or Unverified

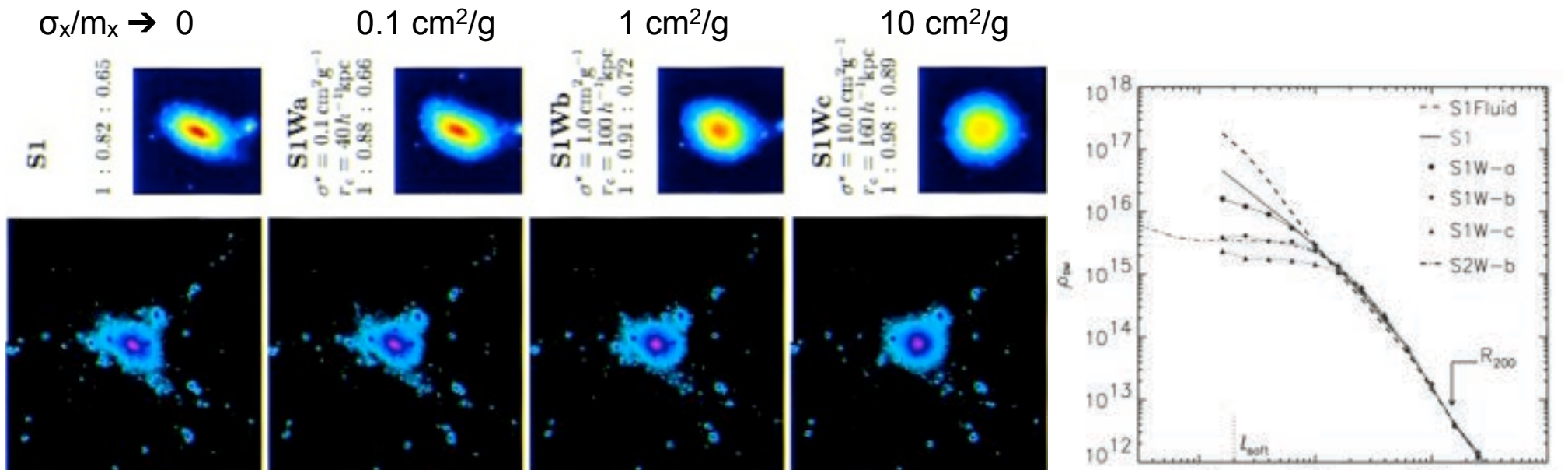
- How is dark matter distributed in cluster & galaxy halos?
 - How centrally concentrated is the DM? Implications for epoch of formation.
 - What degree of substructure exists? and on what scales?
 - How does the DM distribution evolve with time and varies with mass?
 - What correlations exist between the distribution of baryonic matter and DM?
 - Is the DM mass profile universal?
 - Can we constrain the nature of the DM? (is DM collisionless ?)
- How to measure cluster masses and compared them with simulations ? (systematics!)



“Millennium” simulation of DM
(Springel et al. 2005)

The effect of a collisional DM on cluster density profiles

- The presence of a non-negligible self-scattering DM cross section leads to the formation of less cuspy and more spherical cores (Spergel&Steinhardt 2000)
 - ▶ $\sigma_x/m_x \lesssim 0.02 \text{ cm}^2/\text{g}$ (Miralda-Escude 2000) from lack of spherical core in cluster MS2137 (note that the Bullet cluster implies only $\sigma_x/m_x \lesssim 1 \text{ cm}^2/\text{g}$)
 - ▶ $\sigma_x/m_x \lesssim 0.1 \text{ cm}^2/\text{g}$ from the presence of cores with $r_c \lesssim 40h^{-1} \text{ kpc}$ (Yoshida et al. 2000)
 - ▶ $\sigma_x/m_x \lesssim 0.01\text{-}0.6 \text{ cm}^2/\text{g}$ (Firmani et al. 2000) $\frac{\sigma}{m_x} \lesssim 0.2 \text{ cm}^2/\text{g} \left(\frac{0.02 M_\odot \text{pc}^3}{\rho} \right) \left(\frac{100 \text{ km/s}}{v_0} \right)$
 $(\tau_{\text{coll}} \sim 1/n\sigma v = H_0^{-1})$
- A systematic study (cluster selection, multi mass probes of the inner core) on a sample of relaxed clusters has never been carried out



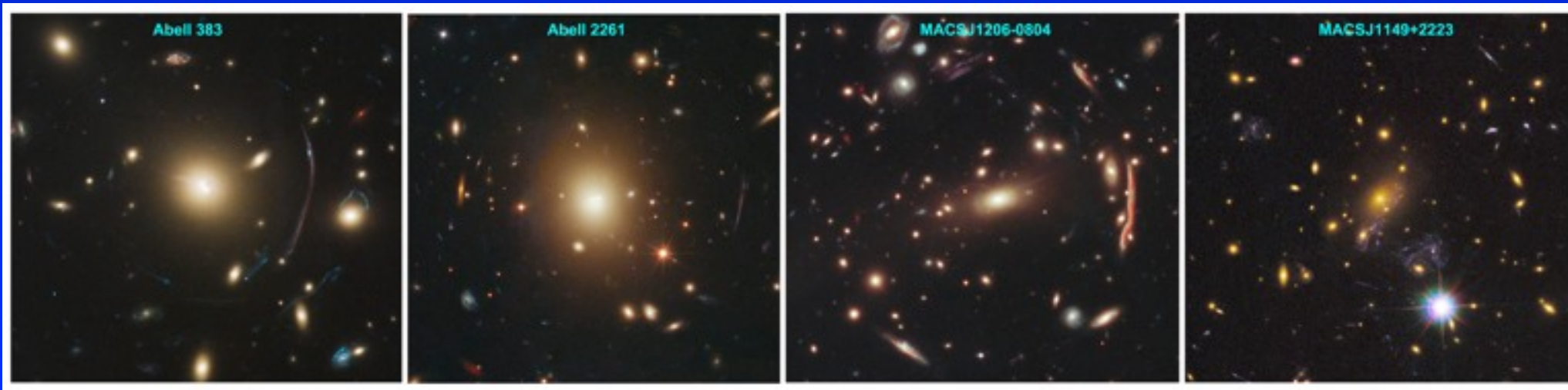
Through a Lens, Darkly:
An Innovative Hubble Survey to Study
the Dark Universe



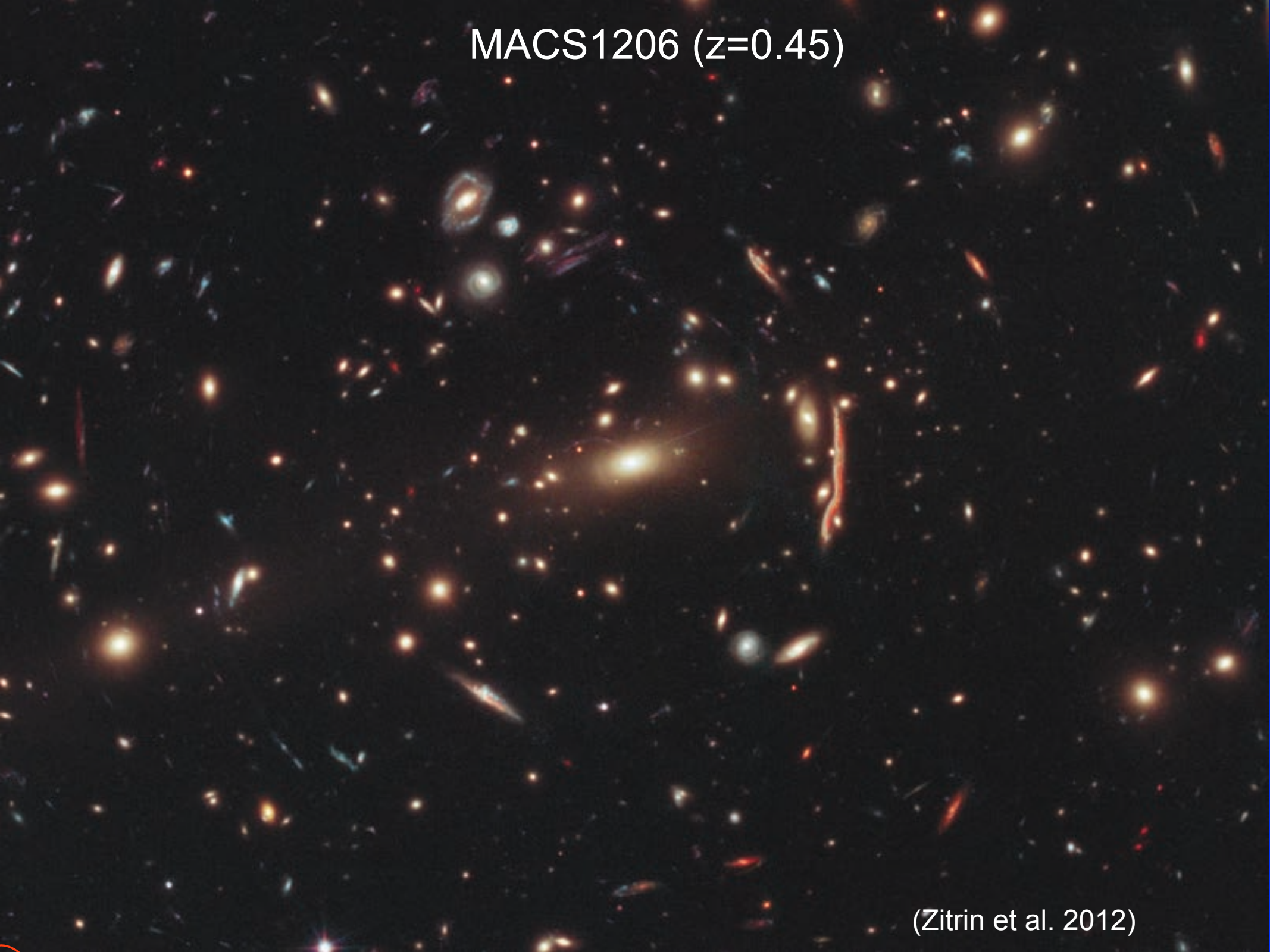
Cluster Lensing And Supernova survey with Hubble

HST multi-cycle Treasury Program (530 orbits) - PI: M.Postman

- Panchromatic (ACS+WFC3 16 filters) imaging of 25 massive intermediate- z galaxy clusters
- Measure DM mass profiles over 10-3000 kpc with unprecedented precision
- “Wide-field” gravitational telescopes on the very high- z Universe
- SNe Ia search at $1 < z < 2$ from parallel fields (doubling SNe at $z > 1.2$), combined w/ CANDELS
- Coordination with a wide range of facilities (Subaru imaging, VLT spec, Spitzer, Chandra/XMM, SZ,..)



MACS1206 ($z=0.45$)



(Zitrin et al. 2012)



(Zitrin et al. 2012)

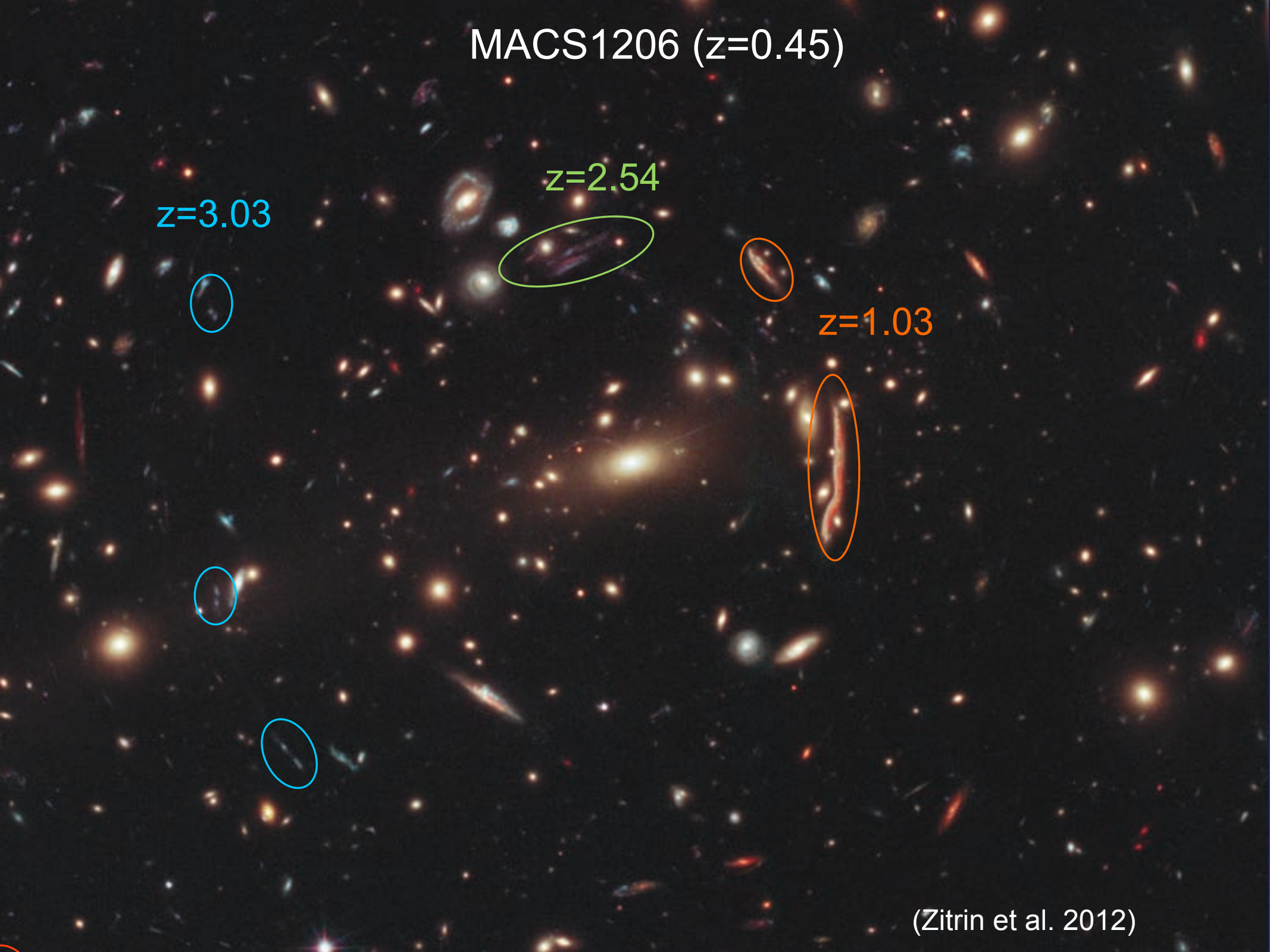
MACS1206 ($z=0.45$)

$z=3.03$

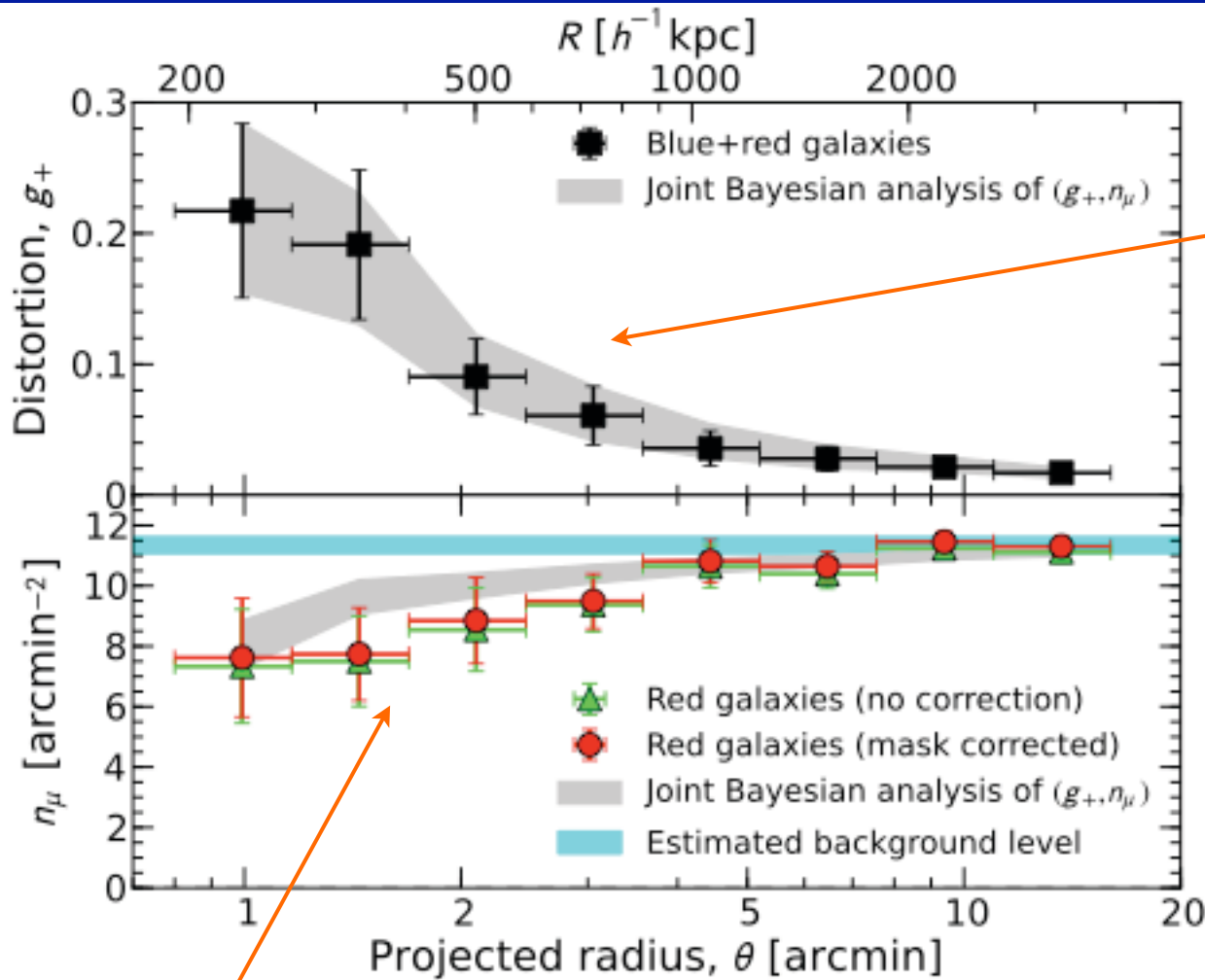
$z=2.54$

$z=1.03$

(Zitrin et al. 2012)



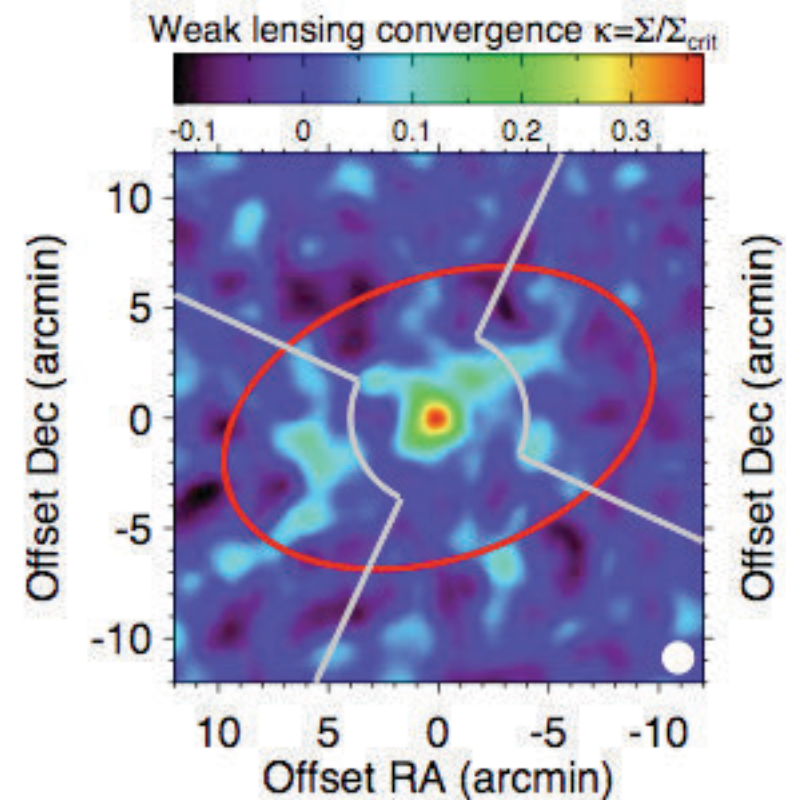
Weak Lensing Analysis of MACS1206 Subaru imaging



Tangential reduced shear

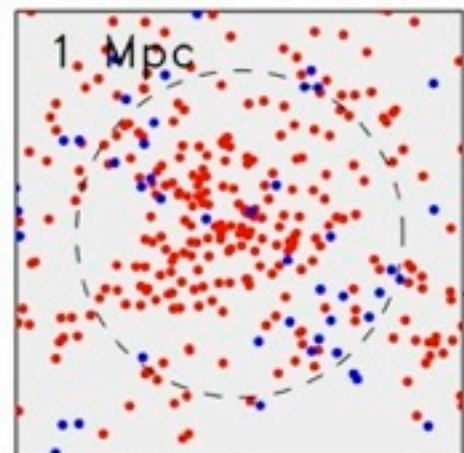
Umetsu et al. 2012

Number counts depletion



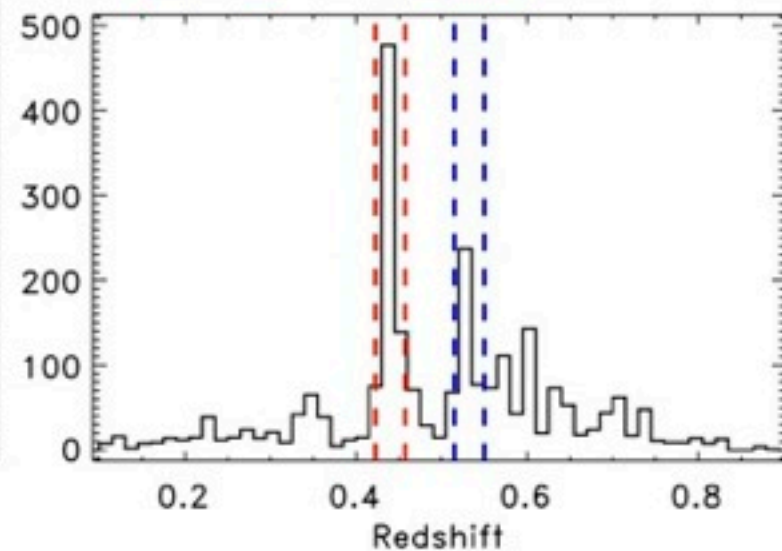
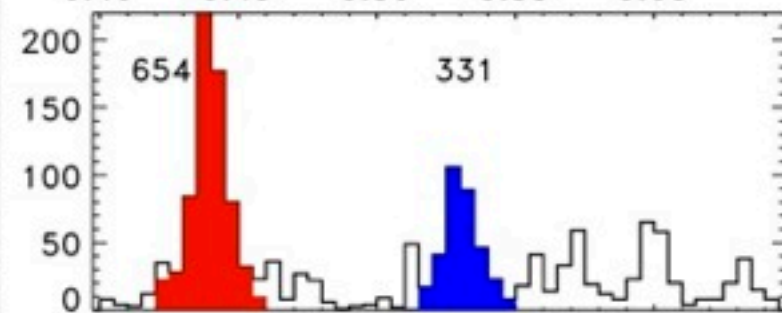
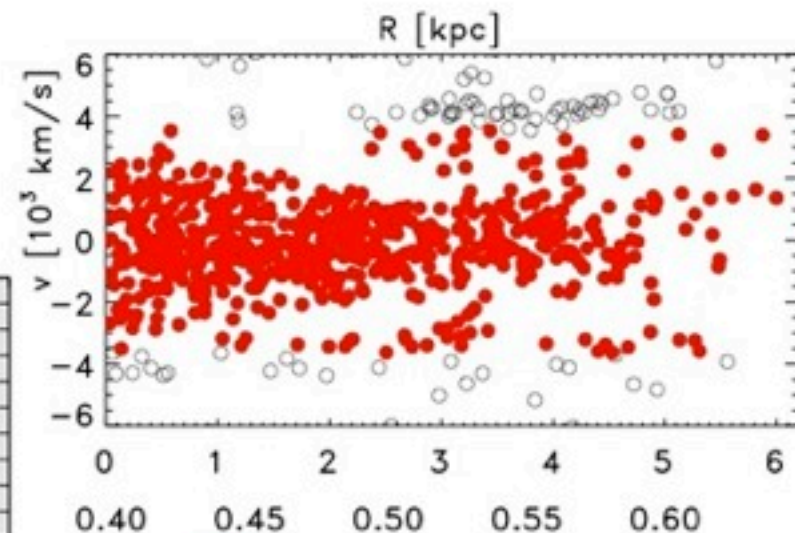
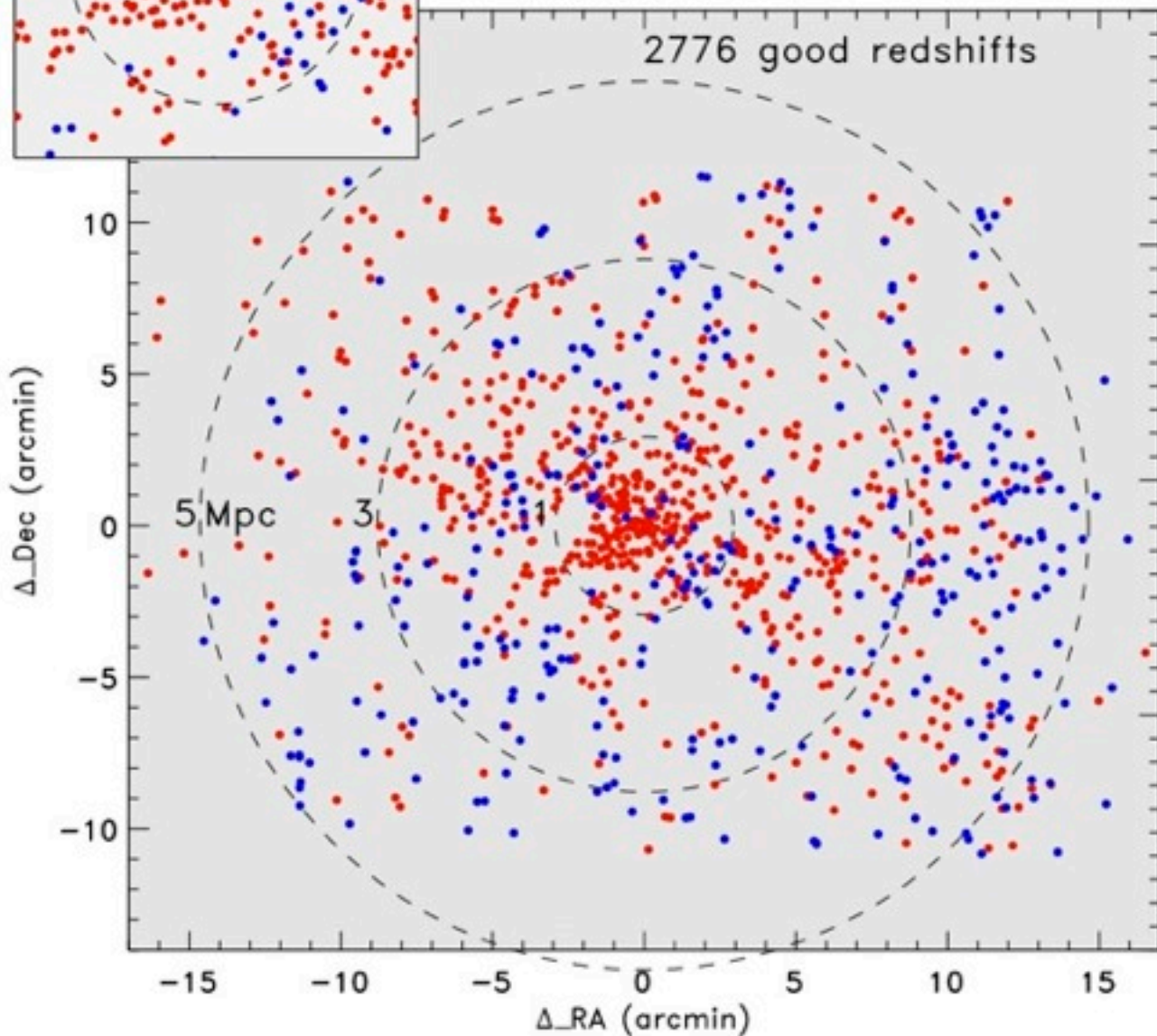
MACS1206: summary

~650 spec members!



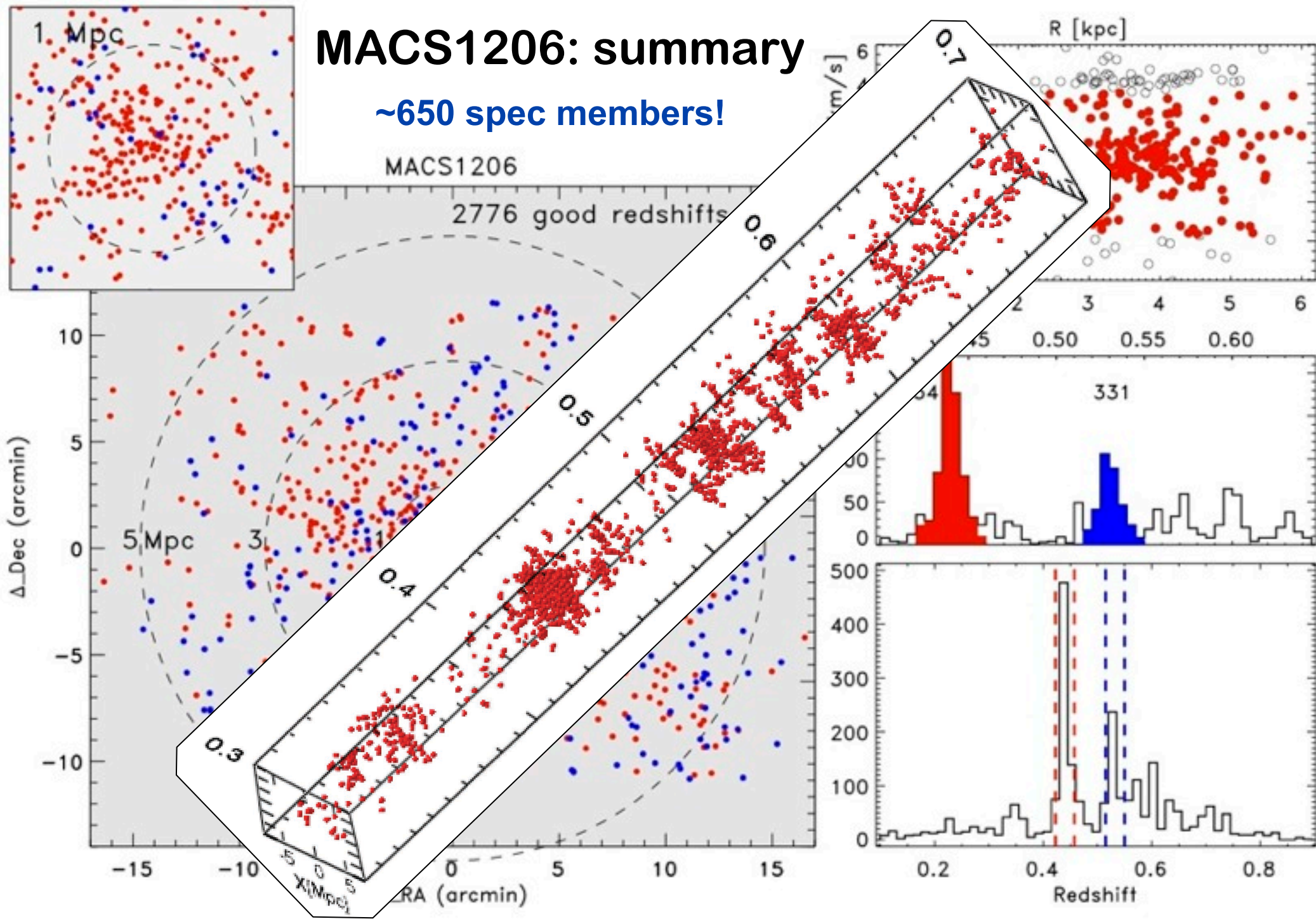
MACS1206

2776 good redshifts



MACS1206: summary

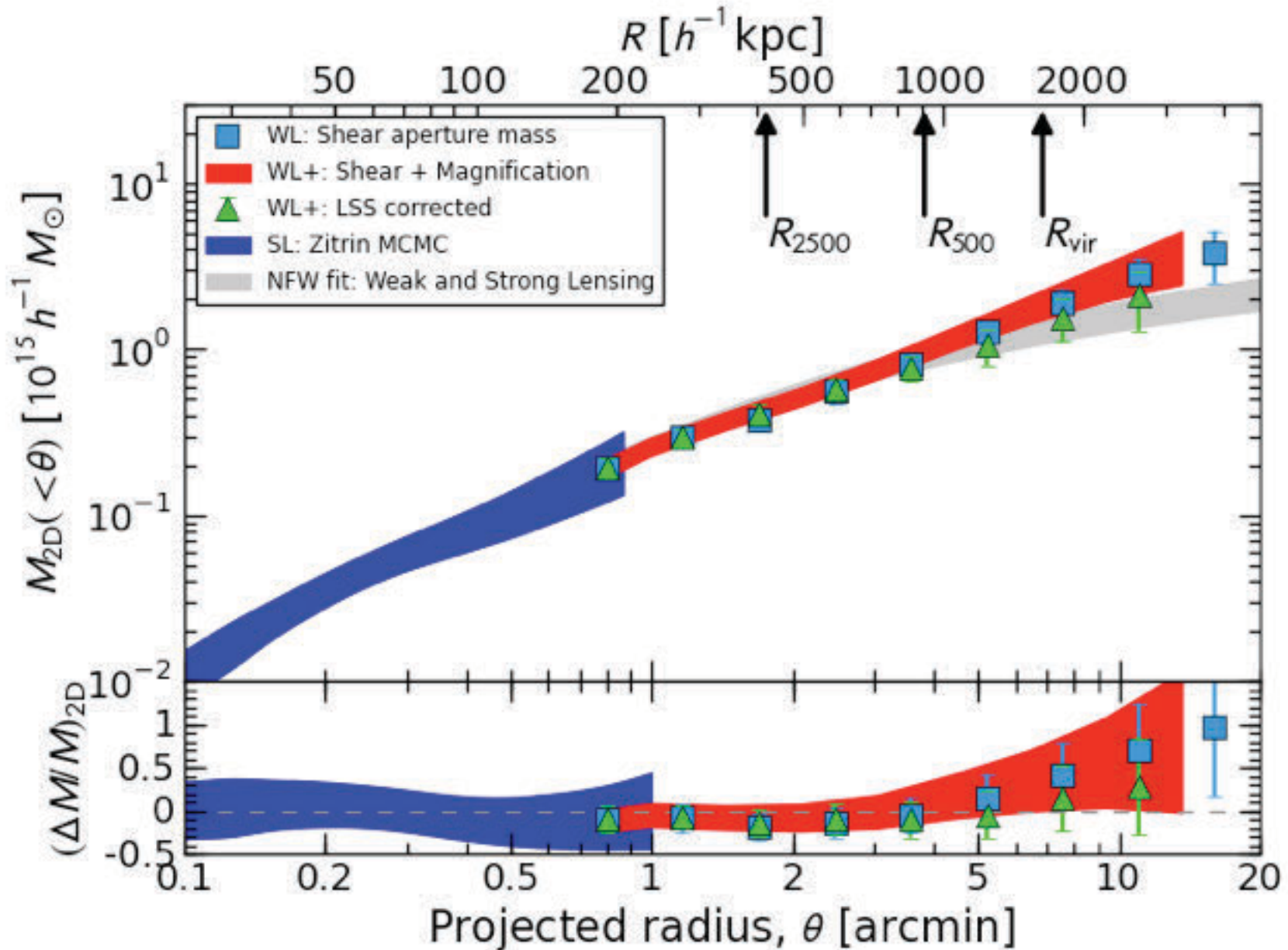
~650 spec members!



MACS1206 ($z=0.45$)

Total mass profile from completely independent methods

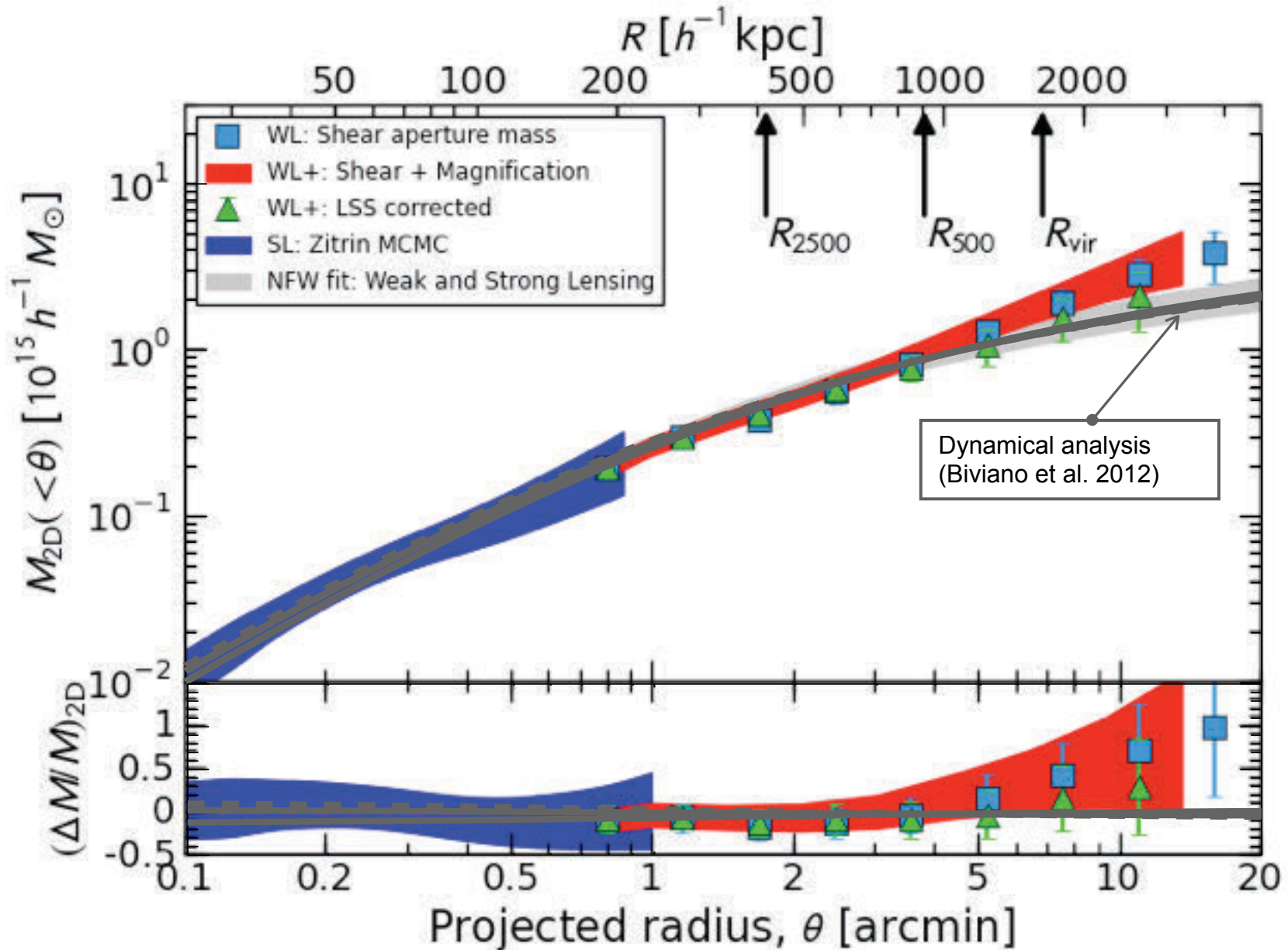
(Umetsu & CLASH team 2012)



MACS1206 (z=0.45)

Total mass profile from completely independent methods

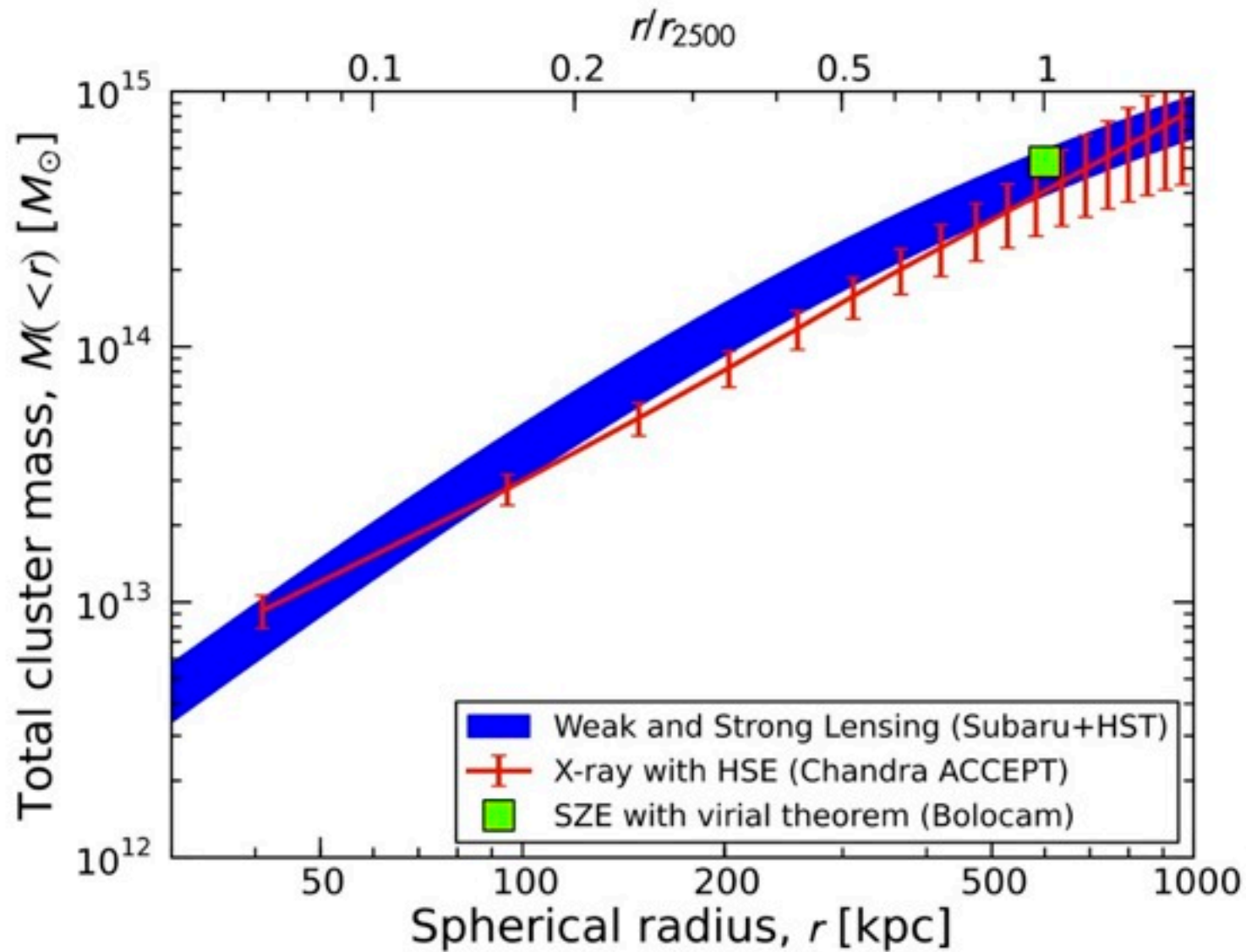
(Umetsu & CLASH team 2012)



Total 3D spherical mass

X-ray vs lensing mass profile

(Umetsu & CLASH team 2012)



Concentration – Total Mass Relationship from CLASH

(D.Coe & CLASH team 2012)

